

This Page Is Inserted by IFW Operations
and is not a part of the Official Record

BEST AVAILABLE IMAGES

Defective images within this document are accurate representations of the original documents submitted by the applicant.

Defects in the images may include (but are not limited to):

- BLACK BORDERS
- TEXT CUT OFF AT TOP, BOTTOM OR SIDES
- FADED TEXT
- ILLEGIBLE TEXT
- SKEWED/SLANTED IMAGES
- COLORED PHOTOS
- BLACK OR VERY BLACK AND WHITE DARK PHOTOS
- GRAY SCALE DOCUMENTS

IMAGES ARE BEST AVAILABLE COPY.

**As rescanning documents *will not* correct images,
please do not report the images to the
Image Problem Mailbox.**



IN THE UNITED STATES PATENT AND TRADEMARK OFFICE

Applicant : Shimon Sakaguchi Art Unit : 1632
Serial No. : 09/284,114 Examiner : Michael C. Wilson
Filed : April 7, 1999
Title : A MOUSE STRAIN WITH NATURAL ONSET OF AUTOIMMUNE
ARTHRITIS

Commissioner for Patents
P.O. Box 2327
Arlington, VA 22202

DECLARATION UNDER 37 C.F.R. §1.132

1. I, Shimon Sakaguchi, Ph. D., having an address at Higashi-hiraki-cho 20, Takano, Sakyo-ku, Kyoto 606-8107, Japan, am the sole inventor of the above-referenced United States patent application serial no. 09/284,114. I am a professor of Experimental Pathology at the Institute for Frontier Medical Sciences, Kyoto University, and am an expert in the general fields of experimental pathology and immunology, particularly, in the field of arthritis.

2. On November 6, 2001, I deposited a stable strain of mice that developed rheumatoid arthritis with the International Patent Organism Depository National Institute of Advanced Industrial Sciences and Technology. The deposit, received on November 6, 2001, was accepted by the International Depository Authority and assigned accession number FERM BP-7790.

3. The deposited material is the same as that described in the specification on page 3, lines 6-7, see the reference to the SKG strain. The SKG strain was first described in Japanese priority application no. 267126/1996, filed October 8, 1996. The deposited mouse embryos were obtained from SKG mice that were owned and in my custody at the time of filing of the priority application, at the time of filing of the present application, and remain in my custody today. I submit that this strain is the

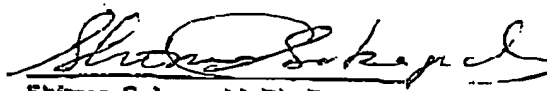
same as that deposited on November 6, 2001, with the International Depository Authority.

4. Accordingly, I submit that the deposited material, FERM BP-7790, was in my possession at the time of filing of the instant application, that the deposited material is the same material as that described in the specification as the SKG strain and that the SKG strain is currently in my possession.

5. I hereby declare that all statements made herein of my own knowledge are true and that all statements made on information and belief are believed to be true; and further that these statements were made with the knowledge that willful false statements and the like so made are punishable by fine or imprisonment, or both, under Section 1001 of Title 18 of the United States Code and that such willful false statements may jeopardize the validity of the application or any patents issued thereon.

Respectfully Submitted

Date: May 19, 2004



Shimon Sakaguchi, Ph. D.

Professor

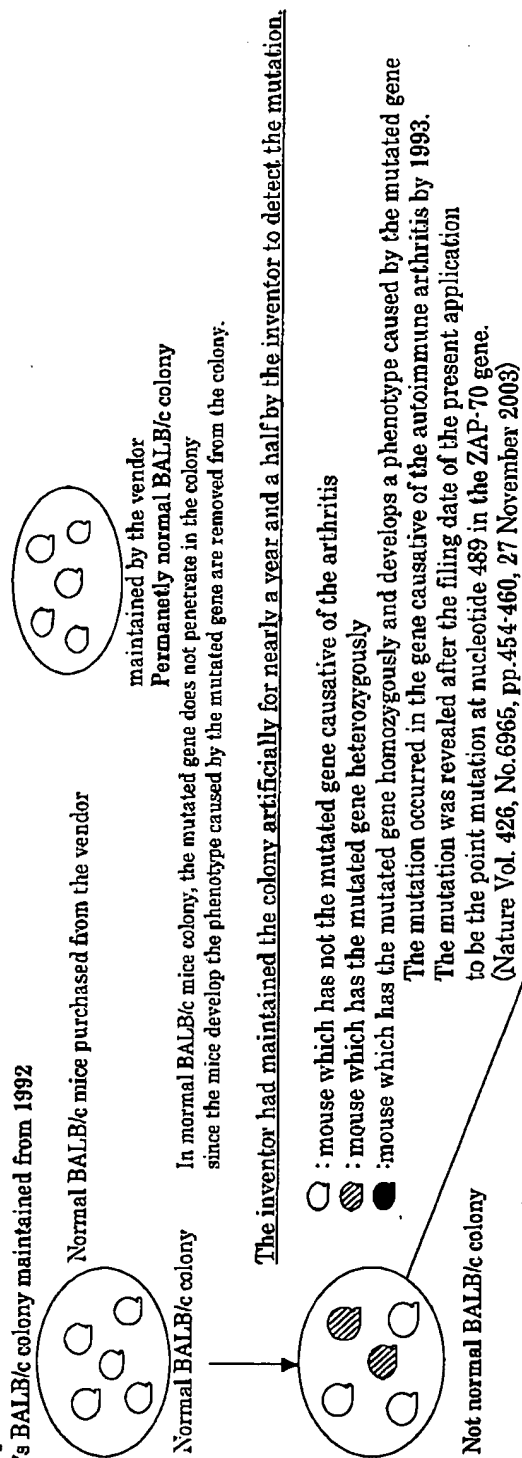
Department of Experimental Pathology

Institute for Frontier Medical Sciences

Kyoto University



Figure 1-1
Inventor's BALB/c colony maintained from 1992



The first mating experiment

The first mating experiment was carried out in 1993.

The female mouse (founder) having the arthritis was found in 1993.

The founder was created by the inventor's effort to maintain the colony artificially for a long time.

The mouse had the mutated gene homozygously.

It was deduced that the mutated genes were penetrated in the colony.

The gene causative of the arthritis gradually penetrated in the colony since the colony was maintained artificially by the inventor.

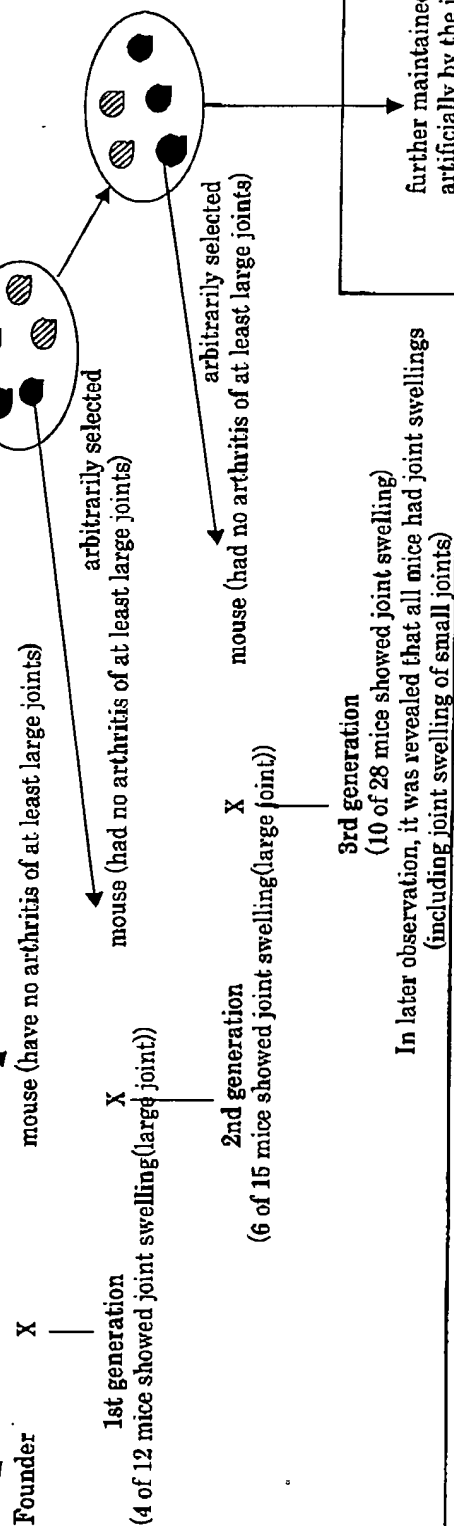
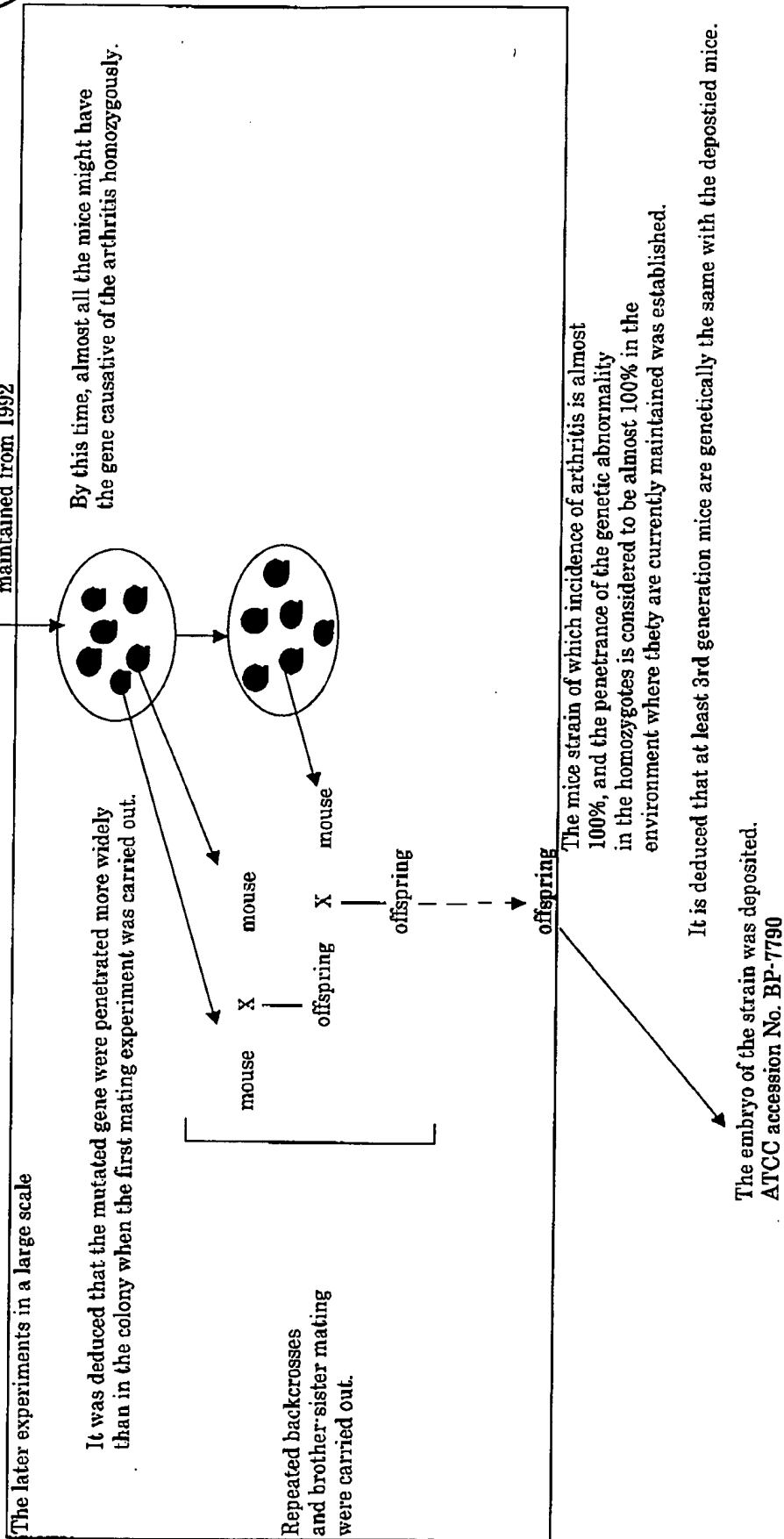




Figure 1-2



The inventor reported about the SKG mice in NATURE on November 27, 2003.
The SKG strain was authorized to be a novel strain.

T LYMPHOCYTES ARE NOT REQUIRED FOR THE SPONTANEOUS DEVELOPMENT OF ENTHESEAL OSSIFICATION LEADING TO MARGINAL ANKYLOSIS IN THE DBA/1 MOUSE

ALEXANDRE CORTHAY, ANN-SOFIE HANSSON, and RIKARD HOLMDAHL

Objective. Male mice of the DBA/1 inbred strain spontaneously develop polyarthritis and toe stiffness when they are ≥ 4 months old. The arthritis affects predominantly the proximal interphalangeal joints and the ankle of the hind limbs. The current study was aimed at determining the importance of T lymphocytes in this disease.

Methods. Histologic sections of hindpaws from arthritic DBA/1 mice were examined. The role of T lymphocytes was studied by using mice lacking either α/β or γ/δ T cells due to a deletion in T cell receptor β (TCR β) or TCR δ genes.

Results. Arthritis was associated with a massive proliferation of connective tissue (fibroblasts) in synovium and adjacent tissues. Chondroid and bone tissue outgrowth at the entheses generated periarticular osteophytes (enthesophytes) which were deposited on the unchanged margins of the preexisting bone. In some cases, the enthesophytes enlarged enough to bridge and fuse the bones by marginal ankylosis. Articular cartilage was essentially unaffected. Abnormal chondroid tissue formation was common in stiffened toes, suggesting that the same pathology may underlie both joint stiffness and arthritis. Dividing chondrocytes were commonly seen in tendons, but without correlation with arthritis or toe stiffness. Mice lacking α/β or γ/δ T cells developed arthritis at the same incidence as control littermates.

Conclusion. The naturally occurring arthritis in male DBA/1 mice is a T cell-independent enthesopathy characterized by periarticular hyperostosis and mar-

ginal ankylosis. This suggests that the ossification leading to peripheral ankylosis of the joints in human enthesopathies, such as diffuse idiopathic skeletal hyperostosis and seronegative spondylarthropathies, is a T cell-independent process.

Animal models provide unique experimental opportunities to increase our understanding of human arthritis. Erosive arthritis can be induced in susceptible mouse strains by immunization with type II collagen in adjuvant (1). This experimental disease, collagen-induced arthritis (CIA), is a widely used animal model for rheumatoid arthritis (RA). The first study of murine CIA used male DBA/1 mice, which were found to be highly susceptible, and currently, most CIA experiments are performed with male DBA/1 mice. The DBA/1 strain has not been selected for development of arthritis or other autoimmune diseases and is one of the most commonly used mouse strains. However, in addition to their high susceptibility to induction of arthritis, male DBA/1 mice have also been found to develop arthritis spontaneously, i.e., without immunization, when they are >3 months old (2,3). This model of naturally occurring arthritis is of particular interest, since the DBA/1 strain is not known to have any immunologic aberrations or other pathologic defects. This is in contrast to other mouse strains that develop spontaneous arthritis, e.g., the MRL-*lpr/lpr*, Biozzi, and NZB/KN strains (4-6). The high susceptibility of DBA/1 males to both CIA and spontaneous arthritis has raised the possibility of a common pathologic mechanism (2).

We have recently demonstrated, in studies of T cell-deficient mice, that CIA development requires the presence of α/β T cells (7). The present study used the same approach to investigate the role of T cells in spontaneous arthritis in the DBA/1 mouse. We found that spontaneous arthritis, in contrast to CIA, does not require T cells. The pathology of spontaneous arthritis

Supported by grants from the Swedish Medical Research Council, the Swedish Rheumatism Association, King Gustaf V's 80-Year Foundation, and the Koek and Österlunds Foundations.

Alexandre Corthay, MS, Ann-Sofie Hansson, MD, Rikard Holmdahl, MD, PhD: Lund University, Lund, Sweden.

Address reprint requests to Rikard Holmdahl, MD, PhD, Lund University, Section for Medical Inflammation Research, Sölvegatan 19, SE-223 62 Lund, Sweden.

Submitted for publication July 8, 1999; accepted in revised form December 1, 1999.

T CELL-INDEPENDENT OSSIFYING ENTHESOPATHY

845

differs dramatically from that of CIA and is primarily an enthesopathy characterized by the formation of periarticular osteophytes.

MATERIALS AND METHODS

Mice. Two male mice, with a mixed (129 × C57Bl/6) background, that selectively lacked either α/β or γ/δ T cells as a result of targeted germline mutation in their T cell receptor (TCR) β or δ genes, respectively (8,9), were purchased from Jackson Research Laboratories (Bar Harbor, ME). The mutated TCR loci were backcrossed onto the DBA/1 background (originating from Jackson Research Laboratories) for 6–7 generations. Subsequent intercrossing of mice that were either heterozygous or homozygous for a mutated TCR generated both homozygous (α/β or γ/δ T cell deficient) and heterozygous (with normal T cell phenotypes) offspring littermates. The different T cell phenotypes were determined by flow cytometry analysis of blood cells, using monoclonal antibodies specific for either TCR α/β (H57-S97) or TCR γ/δ (GL3) as previously described (7).

Mice were bred and kept in the animal facility of the Section for Medical Inflammation Research at Lund University. Mice were housed in polystyrene cages containing wood shavings and fed standard rodent chow and water ad libitum. Mice were kept in a climate-controlled environment with 12-hour light/dark cycles. Mice were screened for pathogens by the National Veterinary Institute (Uppsala, Sweden) and were found to be positive for intestinal pinworms (*Aspicularis teraperta*) and negative for all viral (lymphocytic choriomeningitis virus, mouse hepatitis virus, minute virus of mice, mouse parvovirus, pneumonia virus of mice, reovirus type 3, and Sendai virus) and bacterial (*Bordetella bronchiseptica*, *Citrobacter freundii* 4280, *Corynebacterium kutscheri*, *Pasteurella* species, *Salmonella*, *Streptococcus β -haemolyticus*, and *Streptococcus pneumoniae*) infections. All animal experiments were approved by an appropriate ethics committee.

Clinical evaluation of arthritis. Mice were examined 1–2 times a week for development of arthritis or toe stiffness. The degree of toe stiffness was assessed by the ability of the mouse to cling (by curling its toes) to a wire grid (the cage lid). This stiffness could be either partial or complete. We classified a toe as stiff when no flexion could be seen for both proximal interphalangeal (PIP) joints and distal interphalangeal joints.

Histologic preparations. Paws were fixed in 4% formaldehyde solution, decalcified for 2–3 weeks in an EDTA solution, and embedded in paraffin. Sections of 6 μ m were stained with either fast green and Safranin O or hematoxylin and erythrosin.

Statistical analysis. Comparison of data between the groups was performed by Fisher's exact test (for incidence) or by the Mann-Whitney U test (for mean day of age at onset). P values less than 0.05 were considered significant.

RESULTS

Macroscopic evaluation of the spontaneous arthritis in male DBA/1 mice. Our laboratory has previously reported that the spontaneous development of

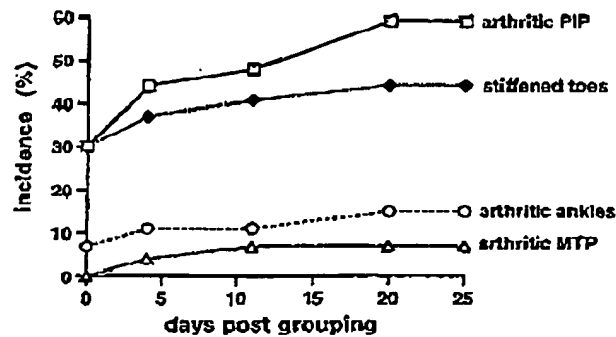


Figure 1. Spontaneous development of arthritis and toe stiffness in male DBA/1 mice. Twenty-seven adult DBA/1 male mice (ages 6–9 months) from 7 cages were grouped 9/cage on day 0 and examined for 25 days. Shown are the incidences of arthritis in the hind proximal interphalangeal (PIP), ankle, or metatarsophalangeal (MTP) joints, as well as the incidence of stiffened toes.

arthritis in male DBA/1 mice is influenced by both hormonal and behavioral factors (3). In particular, the number of mice in each cage is critical, with ≥ 3 males/cage required for development of arthritis (3). It was found that grouping of sexually mature males from different litters effectively increased both arthritis incidence and severity, as evaluated by the number of affected joints (3). Random grouping of the litters was used to standardize the mice in each cage and thus reduce the otherwise rather high variations in disease incidence between cages.

In a first experiment, 27 DBA/1 males (ages 6–9 months) from 7 cages were grouped 9/cage, and arthritis was macroscopically evaluated once a week (Figure 1). Development of arthritis was seen in the PIP, the ankle, and the metatarsophalangeal (MTP) joints of the hind limbs, with the PIP joints most affected and the MTP joints least affected (Figure 1). Arthritis in the PIP joint (Figure 2D) started with a typical joint swelling and erythema. The erythema was apparent for several weeks (range 1–10) and then tended to disappear, leaving the joint larger and deformed. Arthritis in the ankle resulted in a typical ankle deformity (Figure 2E). Toe stiffness, assessed by placing the mouse on a wire grid (Figure 2F) was commonly seen in the hindpaws (Figure 1).

Histopathology of arthritic paws. For histologic analysis, 6 of 16 arthritic mice (ages 8–10 months) were randomly chosen at the end of the first experiment (i.e., 25 days after grouping; see Figure 1). Each of the 6 chosen mice had at least 1 arthritic PIP joint, and 4 of these mice had stiffened toes.

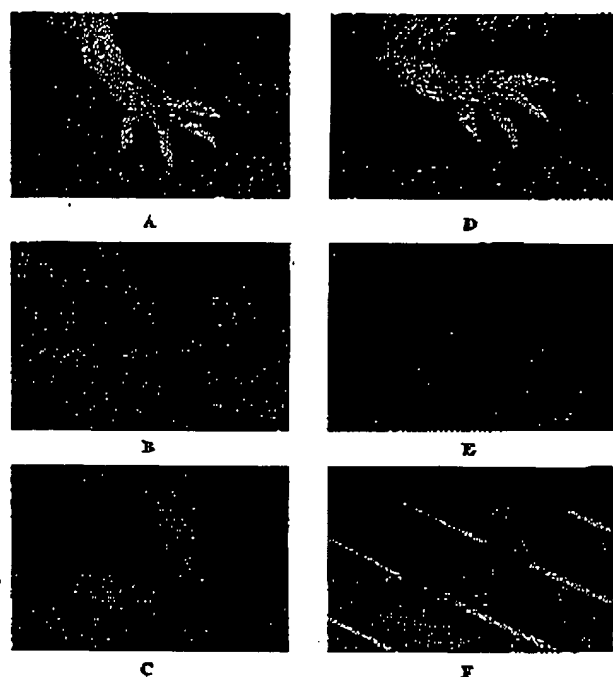


Figure 2. Spontaneous arthritis and toe stiffness in male DBA/1 mice. Shown are a typical arthritic toe (D), arthritic ankle (arrow in E), and stiff toe (arrow in F), while A-C show normal paws. All mice were 6 months old.

A systematic histologic evaluation of the hind PIP joints is shown in Table 1. In 86% of the arthritic toes, histopathologic analysis revealed a proliferation of connective tissue (fibroblasts) in synovium and adjacent tissue (Figure 3 and Table 1). Formation of a chondroid nodule by proliferation of chondrocytes was commonly

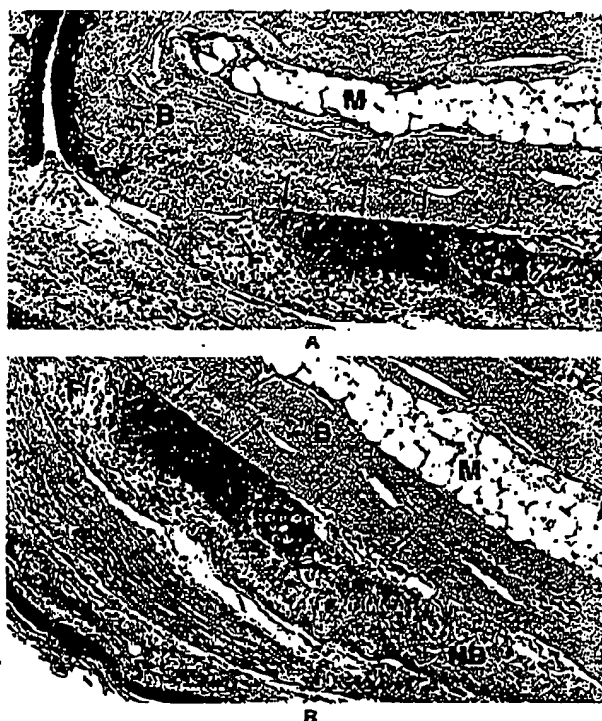


Figure 3. Early histologic changes in the proximal interphalangeal joints of wild-type DBA/1 male mice with spontaneous arthritis. A and B show typical early changes, with fibroblast proliferation in synovium and adjacent tissues, and formation of a chondroid nodule by proliferation of chondrocytes in the enthesis. Note the unchanged margins of the preexisting bone (arrows) and the unaffected articular cartilage. New bone formation at the enthesis is apparent in B. (Safranin O and fast green-stained sections of an 8-month-old mouse; original magnification $\times 100$.) B = bone; C = articular cartilage; F = fibroblasts; M = bone marrow; NB = new bone; NC = new cartilage.

Table 1. Histologic evaluation of proximal interphalangeal (PIP) joints of the hind limbs of male DBA/1 mice*

Macroscopic appearance of PIP joint	Fibroblast proliferation	Chondroid tissue			Enthesal new bone formation	Normal
		In enthesis	In tendon	Total		
Arthritic (n = 7)	6 (86)†	6 (86)†	1 (14)	7 (100)†	4 (57)†	0 (0)†
Stiffened (n = 15)	2 (13)‡	6 (40)	4 (27)	10 (67)	5 (33)	5 (33)
Normal (n = 24)	0 (0)	3 (13)	5 (21)	8 (33)	2 (8)	16 (67)

* Hind PIP joints from 6 male DBA/1 mice (ages 8-10 months) were macroscopically examined and classified into 1 of the following groups: arthritic, stiffened, or normal. All 6 mice had at least 1 arthritic PIP joint, and 4 of them had stiffened toes. Histologic sections of the toes were analyzed by a blinded observer, and 46 of 48 PIP joints (great toes excluded) were evaluated and are represented here. The 2 remaining PIP joints (not shown) were clinically scored as normal (their histologic preparations were incomplete). Values are the number of affected PIP joints in each group for each histologic feature observed (percent of the total number of joints in each group).

† $P < 0.05$ compared with normal-joints group (by Fisher's exact test).

‡ $P < 0.05$ compared with arthritic-joints group (by Fisher's exact test).

T CELL-INDEPENDENT OSSIFYING ENTHESOPATHY

847

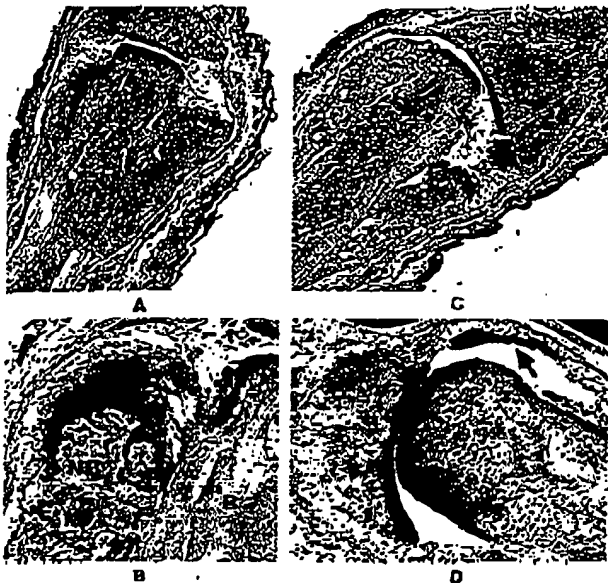


Figure 4. Late histologic changes in the proximal interphalangeal joints of wild-type DBA/1 male mice with spontaneous arthritis. A-C, Formation of periarticular enthesophytes consisting of a central core of bone (with marrow) capped by proliferating cartilage at the surface. C, Fusion of enthesophytes resulting in marginal ankylosis and lateral deviation of the distal phalanx. D, Proliferation of chondrocytes in a tendon (arrow). (Safranin O and fast green-stained sections of 8-10-month-old mice; original magnification $\times 25$ in A and C; $\times 100$ in B and D.) B = bone; C = articular cartilage; M = bone marrow; NB = new bone; NC = new cartilage.

observed in the enthesis, the region where the joint capsule and ligaments attached to the bone (Figure 3 and Table 1). The newly formed chondrocytes appeared to originate from periosteal fibroblasts which became enlarged and rounded (Figure 3). The chondroid tissue formation in the enthesis was often accompanied by new bone formation (Figure 3B). This suggested that the chondrocytes either differentiated into osteocytes or, alternatively, that osteocytes were progressively replacing the chondrocytes through endochondral ossification. The newly formed chondroid and bone tissue was deposited on the unchanged margins of the preexisting bone, indicating that the old bone was only used as a template (Figure 3). The cell proliferation in the enthesis resulted in formation of periarticular osteophytes (enthesophytes), consisting of a central core of bone capped by proliferating cartilage at the surface (Figures 4A-C). The enthesophytes, which often contained bone marrow, could in some cases enlarge to bridge and fuse

the joint by marginal ankylosis (Figure 4C). During the entire process of enthesal ossification, the articular cartilage was essentially unaffected.

Proliferation of chondrocytes was occasionally seen in tendons (Table 1 and Figure 4D), but this histologic feature appeared asymptomatic, since it was not associated with macroscopic arthritis or toe stiffness (Table 1). Histopathology of the toes that were macroscopically scored as stiff revealed abnormalities similar to those of the arthritic toes, with proliferation of chondrocytes at the enthesis and new bone formation seen in 33-40% of joints (Table 1). This indicated that the same pathologic mechanisms might have caused both joint stiffness and arthritis. Histology of arthritic ankles also revealed changes similar to those of the arthritic toes, with the characteristic formation of periarticular enthesophytes of cartilage and bone (Figure 5A). Importantly, very few lymphocytes and no polymorphonuclear leukocytes were seen in histologic sections of arthritic joints.

Spontaneous arthritis in T cell-deficient mice. DBA/1 littermate mice were produced that were either heterozygous ($\beta+/-$) or homozygous ($\beta-/-$) for a mutated TCR β chain, or that were either heterozygous ($\delta+/-$) or homozygous ($\delta-/-$) for a mutated TCR δ chain. It was previously reported that homozygotes lacked either α/β ($\beta-/-$) or γ/δ ($\delta-/-$) T cells, while heterozygotes had normal T cell subsets and were indistinguishable phenotypically from wild-type (+/+) mice (7-10).

The spontaneous development of arthritis was

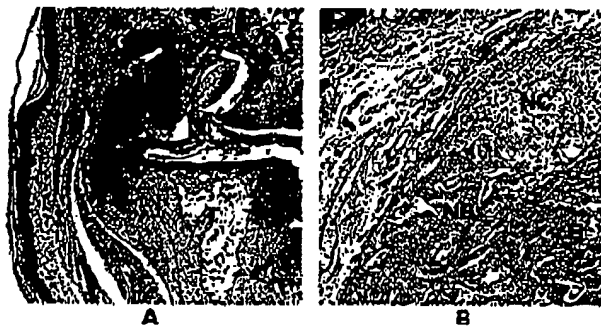


Figure 5. Histology of spontaneous arthritis in male DBA/1 mice. A, Enthesophyte formation on the calcaneus of a wild-type, 10-month-old mouse (Safranin O and fast green-stained section; original magnification $\times 25$). B, Enthesophyte formation in the proximal interphalangeal joint of an α/β T cell-deficient, 7-month-old mouse (hematoxylin and erythrosin-stained section; original magnification $\times 100$). B = bone; NB = new bone; NC = new cartilage.

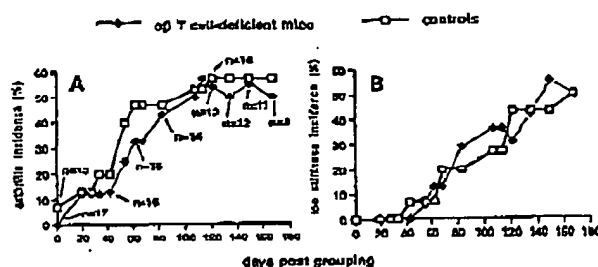


Figure 6. Spontaneous arthritis and toe stiffness development in mice deficient in α/β T cells compared with normal littermates. Adult mice ages 5-13 weeks (α/β T cell-deficient [$n = 17$] and normal littermates [$n = 15$]) were grouped 10-11/cage and examined for 24 weeks. A, Incidence of arthritic toes (affected mice/total number of mice in each group). B, Incidence of stiffened toes (affected mice/total number of mice in each group). No statistically significant difference (by Fisher's exact test) was observed between the groups at any time point.

evaluated in either α/β or γ/δ T cell-deficient mice compared with the phenotypically normal heterozygous littermates. Figure 6 shows the results of an experiment in which α/β T cell-deficient mice ($\beta^{-/-}$) were compared with normal ($\beta^{+/-}$) littermates for the development of arthritis and toe stiffness. No significant difference in the disease course was observed between the 2 groups concerning incidence of arthritic or stiff toes over time. The high mortality observed among α/β T cell-deficient mice (Figure 6A) was most probably due to their severe immunodeficiency and their propensity to spontaneously develop inflammatory bowel disease (11). Histologic sections of paws from arthritic α/β T cell-deficient mice were examined and found to be indistinguishable from those of arthritic wild-type mice (Figure 5B). Figure 7 shows the results of an experiment in which γ/δ T cell-deficient mice ($\delta^{-/-}$) were compared with normal ($\delta^{+/-}$) littermates for the development of arthritis and toe stiffness. No significant difference in the disease course was observed between the 2 groups concerning incidence of arthritic or stiff toes over time. The lack of either α/β or γ/δ T cells did not significantly affect the mean day of disease onset, the mean age at disease onset, or the incidence of arthritis or toe stiffness (Table 2).

DISCUSSION

Histologic investigation of male DBA/1 mice that spontaneously develop arthritis revealed that the disease is an enthesopathy characterized by fibroblast proliferation and the formation of periarticular enthesophytes of

cartilage and bone. There were no changes detected in articular cartilage and bone, although in some cases the enthesophyte outgrowth resulted in marginal ankylosis. By using TCR mutant mice lacking either α/β or γ/δ T cells, we were able to demonstrate that the spontaneous arthritis in DBA/1 males can be macroscopically difficult to distinguish from CIA. CIA is characterized by erosion of joint cartilage and bone and is strictly α/β T cell dependent (7). We can thus conclude that the spontaneous arthritis in the DBA/1 mouse is very different from CIA in the same strain.

Enthesopathy is common in humans and can accompany many disorders, including inflammatory, traumatic, degenerative, endocrine, and metabolic conditions (12). Inflammatory changes are characteristic of the enthesopathy that accompanies certain rheumatic diseases, particularly seronegative spondylarthropathies (12). In ankylosing spondylitis, the entheses are the primary pathologic site, and entheses are affected in both synovial and cartilaginous articulations, as well as in extraarticular locations. Osseous proliferation produces capsular enthesophytes with progressive ankylosis at the margins of the articulation. These pathologic features are strikingly similar to the spontaneous arthritis in the DBA/1 mouse. There are, however, histologic differences between ankylosing spondylitis and the murine spontaneous arthritis. For instance, in the joints of patients with ankylosing spondylitis, there is cellular infiltration by lymphocytes, plasma cells, and polymorphonuclear leukocytes, with associated erosion of the subligamentous bone, which is not found in the DBA/1

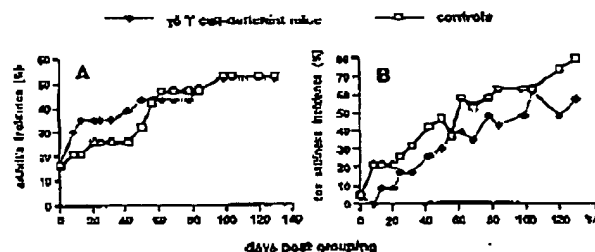


Figure 7. Spontaneous arthritis and toe stiffness development in mice deficient in γ/δ T cells compared with normal littermates. Adult mice ages 11-22 weeks (γ/δ T cell-deficient [$n = 23$] and normal littermates [$n = 19$]) were grouped 10-11/cage and examined for 19 weeks. A, Incidence of arthritic toes (affected mice/total number of mice in each group). B, Incidence of stiffened toes (affected mice/total number of mice in each group). No statistically significant difference (by Fisher's exact test) was observed between the groups at any time point.

T CELL-INDEPENDENT OSSIFYING ENTHESOPATHY

849

Table 2. Spontaneous arthritis and toe stiffness in T cell-deficient male DBA/1 mice*

Experiment, genotype (n)†	Day of onset, mean \pm SD‡			Age at onset, mean \pm SD§			Incidence, %¶		
	Arthritic toes	Stiffened toes	Arthritic ankles	Arthritic toes	Stiffened toes	Arthritic ankles	Arthritic toes	Stiffened toes	Arthritic ankles
Experiment 2									
TCR β +/- (15)	48 \pm 32	99 \pm 42	127 \pm 38	18 \pm 3	25 \pm 6	29 \pm 4	53	47	27
TCR β -/- (17)	64 \pm 36	96 \pm 36	121 \pm 0	19 \pm 5	23 \pm 4	23 \pm 0	47	41	6
Experiment 3									
TCR δ +/- (19)	35 \pm 34	53 \pm 43	90 \pm 45	23 \pm 7	25 \pm 6	31 \pm 6	53	79	37
TCR δ -/- (23)	26 \pm 35	61 \pm 41	78 \pm 0	21 \pm 5	27 \pm 6	32 \pm 3	52	74	9

Protocols for experiments 2 and 3 are described in the legends of Figures 6 and 7. In both experiments, there were no statistically significant differences between the groups for any measured parameter.

T cell receptor (TCR) β -/- mice are deficient in α/β T cells, and TCR δ -/- mice are deficient in γ/δ T cells. TCR β +/- and TCR δ +/- mice are control littermates with wild-type T cell phenotypes.

Day (post grouping) when the first arthritic toe, stiffened toe, or arthritic ankle was observed. Calculations were performed for affected mice only.

Age of the mouse (in weeks) when the first arthritic toe, stiffened toe, or arthritic ankle was observed. Calculations were performed for affected mice only.

Affected mice/total number of mice in each group.

model. This indicates that the etiologies of the diseases may differ.

The joint disorder observed in DBA/1 mice also has similarities to another human disease, diffuse idiopathic skeletal hyperostosis (DISH). The principal manifestation of DISH is ligamentous calcification and ossification of the intercostal aspects of the spinal column, sometimes leading to bony ankylosis (13). DISH frequently involves the peripheral skeletal system, resulting in enthesal ossification and bony spurs (13). DISH affects predominantly males (2:1 male:female ratio), and males appear to be more severely affected (13). In a radiographic study of the hands, prominent enthesopathy with mild or marked new bone formation was seen in all DISH patients investigated (14). In another study, the prevalence of palpable finger joint nodules (Heberden's and Bouchard's nodes) was almost twice as frequent in spinal DISH patients compared with controls (15). This increase was most marked at the 2IP joint and in males (15).

Importantly, DISH seems to occur independently of disc degeneration in the spine (13). Several studies have also found that DISH patients have an increased incidence of obesity, diabetes, hypertension, and gout, suggesting that endocrine and metabolic factors may play a role (13). When we performed whole body radiography of male DBA/1 mice with spontaneous arthritis, there were no changes in the spine (data not shown). This is in contrast to seronegative spondylarthropathies and DISH, which have marked spinal changes. This might be explained by the increased loading of the spine and paraspinal soft tissues in a bipedal species.

In the mouse, 2 spontaneous joint diseases with

similarities to the DBA/1 mouse spontaneous arthritis have been reported, namely, progressive ankylosis and ankylosing enthesopathy (ANKENT). Progressive ankylosis is caused by an autosomal recessive mutation (*ank*), which generates a severe and gradual fusion of the joints in the limbs and axial skeleton (16). The joints first develop a proliferative synovitis, sometimes associated with marginal erosion of the articular cartilage and periosteal bone. Subsequently, cartilaginous enthesophytes bridge the margins of the joint and undergo ossification (16). All mice that are homozygous for the *ank* mutation appear to develop ankylosis, and males and females are equally affected (16). Progressive ankylosis develops in athymic nude (*nu/nu*) mice, and induction of disease by transfer of cells (spleen or bone marrow) or serum has been unsuccessful (17). This strongly indicates that progressive ankylosis is not immune mediated (17). Identification of the mutated gene causing progressive ankylosis will contribute to our understanding of the pathogenesis of ossifying enthesopathy.

ANKENT is a naturally occurring joint disease observed at low frequency in several inbred mouse strains (18). Macroscopically, ANKENT consists of a stiffening of the ankle or tarsal joints. Histology of joints with ANKENT reveals a proliferation of chondrocytes at the entheses, with formation of enthesophytes that may lead to marginal ankylosis (19). ANKENT occurs almost exclusively in males, and grouped caging increases susceptibility to ANKENT (18,20). There are, however, clear differences between the spontaneous arthritis in male DBA/1 mice described here and ANKENT. ANKENT has not been reported to affect toe joints, and

DBA/1 mice were resistant to ANKENT. In contrast, the highest incidence of ANKENT was found in C57Bl strains that are resistant to spontaneous arthritis (3,18). In addition, ANKENT develops several months later than the arthritis described here in DBA/1 mice. Interestingly, HLA-B27 transgene is a relative risk factor for ANKENT (18), but further experiments are required to provide more direct evidence for a role of T cells in ANKENT.

All of the above diseases involved pathologic changes in entheses. Therefore, the critical question is why entheses are so prone to changes, including formation of enthesophytes. Anatomic considerations may be helpful in addressing this issue. Enteses are known to be metabolically active and have a prominent nerve and blood supply (12). In particular, the high vascularity of the enthesis may help explain why endocrine and metabolic conditions preferentially affect this site. In humans, enthesopathy resulting in bone outgrowth is a prominent feature of several endocrine disorders, including diabetes mellitus, acromegaly, and hypoparathyroidism (12). In mice, enthesopathies have been experimentally induced by injection with compounds affecting the cell metabolism, such as retinyl acetate and transforming growth factor β 1 (TGF β 1).

Arthritis was induced in mice of the C3H-A^y strain by daily feeding with high doses of retinyl acetate, a vitamin A derivative (retinoid) (21). Retinyl acetate-induced arthritis affects mainly the hind limbs and consists of the production of enthesophytes and periarticular bony bridging (21). The incidence and severity of arthritis were significantly correlated with the total administered dose of retinyl acetate (21). Retinoids are known to affect the expression of genes and gene products involved with both cellular proliferation and differentiation (21). The mechanism by which retinyl acetate induces the formation of enthesophytes remains to be defined.

Injection of TGF β 1 into the knee joints of male C57Bl/10 mice was reported to induce both chondrocyte proteoglycan synthesis and osteophyte (enthesophyte) formation (22). TGF β 1 plays an important role in cell proliferation and differentiation, as well as in the synthesis and degradation of extracellular matrix (22). High levels of TGF β 1 have been found in affected joints in osteoarthritis and RA patients (22). Consequently, it would be of great interest to test whether similarly high levels of TGF β 1 are present in arthritic joints of DBA/1 mice.

The preponderance of male susceptibility to spontaneous arthritis in DBA/1 mice indicates a role for

sex hormones. Our laboratory has previously shown that no arthritis developed after castration of male DBA/1 mice, and that disease susceptibility was restored by testosterone treatment (3). A number of studies indicate a direct influence of androgens on bone and cartilage cells, and in vitro, androgens can directly stimulate the proliferation of osteoblasts (23). Testosterone has been found to enhance bone formation and calcification in fetal mouse long bone in vitro (24), and testosterone treatment of juvenile frogs (*Xenopus laevis*) induced chondrogenesis in the larynx (25). Consequently, androgens may have a direct role in the generation of enthesophytes in male DBA/1 mice.

Enteses are areas of great stress naturally, and this might obviously play a role in their susceptibility to pathology. Several factors, such as tedious physical activity, overstress, local ischemia, aging, and trauma, have been suggested to cause degenerative enthesopathy and production of enthesophytes (12,15). Spontaneous arthritis in male DBA/1 mice may be influenced by aggressive behavior, leading to stress and trauma in the joints. This is supported by observations that grouped caging enhances the development of spontaneous arthritis. In addition, no arthritis was observed in cages with <3 males or in castrated animals (3). Experiments with partial meniscectomy in rabbits suggested that forces exerted at the site of joint capsule attachment to the bone might play a primary role in osteophyte induction (26). Osteophyte and enthesophyte production may be a compensatory mechanism in the case of joint instability, a hypothesis supported by the fact that marginal osteophytes have been reported to stabilize osteoarthritic knees (27).

In conclusion, the naturally occurring arthritis in DBA/1 male mice is a T cell-independent enthesopathy characterized by periarticular hyperostosis and marginal ankylosis. This suggests that the enthesopathic process leading to peripheral ossification of the joints in human enthesopathies like DISH and seronegative spondylarthropathies is not T cell mediated.

ACKNOWLEDGMENTS

We wish to thank Margareta Svejme for expert help with the histologic preparations, Alexandra Treschow for critical reading of the manuscript, and Lennart Lindström, Carlos Palestro, and Yvette Bärting for taking good care of the animals.

REFERENCES

1. Courtenay JS, Dellman MJ, Dayan AD, Martin A, Mosedal B. Immunization against heterologous type II collagen induces arthritis in mice. *Nature* 1980;283:666-7.

T CELL-INDEPENDENT OSSIFYING ENTHESOPATHY

851

2. Nordling C, Karlsson-Parra A, Jansson L, Holmdahl R, Klareskog L. Characterization of a spontaneously occurring arthritis in male DBA/1 mice. *Arthritis Rheum* 1992;35:717-22.
3. Holmdahl R, Jansson L, Andersson M, Jonsson R. Genetic, hormonal and behavioral influence on spontaneously developing arthritis in normal mice. *Clin Exp Immunol* 1992;88:467-72.
4. Hang L, Theofilopoulos AN, Dixon FJ. A spontaneous rheumatoid arthritis-like disease in MRL/l mice. *J Exp Med* 1982;155:1690-701.
5. Bouvet J-P, Coudere J, Bouthillier Y, Franc B, Ducaillar A, Mouton D. Spontaneous rheumatoid-like arthritis in a line of mice sensitive to collagen-induced arthritis. *Arthritis Rheum* 1990;33:1716-22.
6. Nakamura K, Kashiwazaki S, Takagishi K, Tsukamoto Y, Morohoshi Y, Nakano T, et al. Spontaneous degenerative polyarthritis in male New Zealand black/KN mice. *Arthritis Rheum* 1991;34:171-9.
7. Cortay A, Johansson Å, Vestberg M, Holmdahl R. Collagen-induced arthritis development requires alphabeta T cells but not gamma delta T cells: studies with T cell-deficient (TCR mutant) mice. *Int Immunol* 1999;11:1065-73.
8. Mombaerts P, Clarke AR, Rudnicki MA, Iacomini J, Itohara S, Lafaille JJ, et al. Mutations in T-cell antigen receptor genes alpha and beta block thymocyte development at different stages. *Nature* 1992;360:225-31.
9. Itohara S, Mombaerts P, Lafaille JJ, Iacomini J, Nelson A, Clarke AR, et al. T cell receptor delta gene mutant mice: independent generation of alpha beta T cells and programmed rearrangements of gamma delta TCR genes. *Cell* 1993;72:337-48.
10. Mombaerts P, Mizoguchi E, Ljunggren HG, Iacomini J, Ishikawa H, Wang L, et al. Peripheral lymphoid development and function in TCR mutant mice. *Int Immunol* 1994;6:1061-70.
11. Mombaerts P, Mizoguchi E, Grusby MJ, Glimcher LH, Bhan AK, Taneigawa S. Spontaneous development of inflammatory bowel disease in T cell receptor mutant mice. *Cell* 1993;75:275-82.
12. Rosnick D, Niwayama G. Enteses and enthesopathy: anatomical, pathological, and radiological correlation. *Radiology* 1983;146:1-9.
13. Ustinger PD. Diffuse idiopathic skeletal hyperostosis. *Clin Rheum Dis* 1985;11:325-51.
14. Littlejohn GO, Urowitz MB, Sanyal HA, Keystone EC. Radiographic features of the hand in diffuse idiopathic skeletal hyperostosis (DISH): comparison with normal subjects and acromegalic patients. *Radiology* 1981;140:623-9.
15. Schlappbach P, Beyeler C, Gerber NJ, van der Linden S, Durgi U, Fuchs WA, et al. The prevalence of palpable finger joint nodules in diffuse idiopathic skeletal hyperostosis (DISH): a controlled study. *Br J Rheumatol* 1992;31:531-4.
16. Hakim FT, Cranley R, Brown KS, Eanes ED, Hame L, Oppenheim JJ. Hereditary joint disorder in progressive ankylosis (ank/ank) mice. I. Association of calcium hydroxyapatite deposition with inflammatory arthropathy. *Arthritis Rheum* 1984;27:1411-20.
17. Krug HE, Wiegrefe MM, Ytterberg SR, Tanog JD, Mahowald ML. Murine progressive ankylosis is not immunologically mediated. *J Rheumatol* 1997;24:115-22.
18. Weinreich S, Eulderink F, Capkova J, Pla M, Gaede K, Heesemann J, et al. HLA-B*27 as a relative risk factor in ankylosing enthesopathy in transgenic mice. *Hum Immunol* 1995;42:103-15.
19. Eulderink F, Ivanyi P, Weinreich S. Histopathology of murine ankylosing enthesopathy. *Pathol Res Pract* 1998;194:797-803.
20. Weinreich S, Capkova J, Hoebe-Hewryk B, Boog C, Ivanyi P. Grouped aging predisposes male mice to ankylosing enthesopathy. *Ann Rheum Dis* 1996;55:645-7.
21. Boden SD, Labropoulos PA, Ragsdale BD, Gullino PM, Gerber LH. Retinyl acetate-induced arthritis in C3H-A⁷ mice. *Arthritis Rheum* 1989;32:625-33.
22. Van Boven HM, van der Kraan PM, Arntz OJ, van den Berg WB. Transforming growth factor-beta 1 stimulates articular chondrocyte proteoglycan synthesis and induces osteophyte formation in the murine knee joint. *Lab Invest* 1994;71:279-90.
23. Kasperk CH, Wergedal JE, Farley JR, Linkhart TA, Turner RT, Baylink DJ. Androgens directly stimulate proliferation of bone cells in vitro. *Endocrinology* 1989;124:1576-8.
24. Schwartz Z, Soskolne WA, Neubauer T, Goldstein M, Adi S, Ornoy A. Direct and sex-specific enhancement of bone formation and calcification by sex steroids in fetal mice long bones in vitro biochemical and morphometric study. *Endocrinology* 1991;129:1167-74.
25. Sassoon D, Segal N, Kelley D. Androgen-induced myogenesis and chondrogenesis in the larynx of *Xenopus laevis*. *Dev Biol* 1986;113:135-40.
26. Moskowitz RW, Goldberg VM. Studies of osteophyte pathogenesis in experimentally induced osteoarthritis. *J Rheumatol* 1987;14:311-20.
27. Pottenger LA, Phillips FM, Draganich LF. The effect of marginal osteophytes on reduction of varus-valgus instability in osteoarthritic knees. *Arthritis Rheum* 1990;33:853-8.

Arthritis & Rheumatism and Arthritis Care and Research Available Online

Arthritis & Rheumatism and Arthritis Care and Research are now being published online, under the addresses www.arthritisrheum.org and www.arthritisresearch.org, respectively. Until July 2000, access to the sites will be free; after that time, nonsubscribers will have access on a pay-per-view basis. Subscribers to the print versions of the journals will continue to have free access to the electronic versions as part of their subscription. This will be accomplished with an initial sign-in via the subscriber number from the journal mailing label; subsequently, the subscriber will be able to choose a user name and password. Each issue of the journals will be electronically published in its entirety. The online journals will be linked to each other, to the ACR Web site, and to Medline. Several simple and sophisticated search features will be included. Planned features include linking to other journals with which reciprocal arrangements have been made, linking to other sources, e-alerts for specific content, and use of supplemental color figures in articles.

CONCISE REPORT

Ankylosing enthesitis, dactylitis, and onychoprosperiostitis in male DBA/1 mice: a model of psoriatic arthritis

R J U Lories, P Matthys, K de Vlam, I Derese, F P Luyten

Ann Rheum Dis 2003;63:595-598. doi: 10.1136/ard.2003.013599

Objective: To develop a murine model of spontaneous arthritis in aging male DBA/1 mice as a model for spondyloarthropathy with good phenotypic reproducibility and relevance to human spondyloarthropathy and psoriasis.

Methods and results: Aging male DBA/1 mice from different litters were caged together (six mice per cage) for the age of 12 weeks. In each cage, one mouse was killed at different times. In all cages, mice were dissected and inspected for clinical signs of arthritis. Results: Disease incidence varied between 50% and 100% in different experiments. Radiological signs of arthritis (osteophytes, erosions) were not seen. Pathological signs of arthritis showed the occurrence of dactylitis, dactylitis, and onychoprosperiostitis in 6 of 50 paws examined. Onychoprosperiostitis with progressive destruction of the nail bed and the underlying phalanx was seen in 12 of 50 paws examined.

Conclusion: Although dactylitis and onychoprosperiostitis are rare manifestations of the disease process, these data strongly suggest that spondyloarthropathy in aging male DBA/1 mice is a murine model for spondyloarthropathy and psoriasis. This model may therefore be an important tool to study links between these two inflammatory and autoimmune phenomena, with particular relevance to human psoriatic arthritis.

Psoriatic arthritis (PsA) is a common and destructive chronic inflammatory joint disease with a long term functional outcome that appears to be comparable to rheumatoid arthritis.¹ Specific clinical signs of PsA include ankylosing enthesitis (AE) in the peripheral joints and dactylitis.² Primary enthesitis is suggested to be the characteristic feature.³ Therefore PsA is part of the spondyloarthropathy (SpA) concept.⁴ Psoriatic nail lesions such as onycholysis, formation of subungual oil spots, and pitting nails are often encountered in patients with PsA. Onychoprosperiostitis (OPP) with periosteal cell proliferation and erosion of the distal phalanx is a less common yet pathognomonic sign of PsA.^{5,6}

Spontaneous arthritis in aging male DBA/1 mice (SpAD) is characterised by AE in the peripheral joints of the hind paws. Its pathology is strongly reminiscent of human SpA and PsA in particular.⁷ Despite clinical signs suggesting important joint inflammation,⁸ the specific relevance of this model to human chronic arthritis has been debated, given the absence of inflammatory infiltrates in the synovium⁹ as well as the observation that both T cell receptor α and γ knockout mice develop disease with similar incidence and severity as wild-type mice.¹⁰

We suggested that not all disease manifestations may have been described in this model. A hitherto unrecognised

inflammatory reaction may precede signs of AE. Therefore, we examined mice at different ages with or without symptoms. We report that not only AE but also dactylitis and nail involvement in SpAD are strikingly similar to human SpA and, in particular, to PsA.

MATERIALS AND METHODS

Animal experiments

In four different experiments, 33 male DBA/1 mice from different litters were caged together at the age of 12 weeks (4-6 mice per cage) and checked twice weekly for clinical signs of arthritis. In the first three experiments animals were killed 7 (age 21 weeks, 10 mice) or 8 weeks (age 24 weeks, 2x8 mice) after the first symptoms in the cohort developed. In one experiment the animals were killed 4 weeks after the first signs of disease occurred (age 25 weeks, 7 mice). The local Ethical Committee for Animal Experiments approved the procedures.

Pathology

A complete microscopic analysis of forefoot from the hind paws was performed in 25 animals (experiments 2-4). Mice hind paws were dissected, fixed in formalin for 16 hours, decalcified using Decal (Serva, Heidelberg, Germany) for 72 hours, dehydrated, and embedded in paraffin. Sections were cut in a transversal plane allowing analysis of all interphalangeal and metatarsophalangeal joints. Sections were stained with haematoxylin and eosin.

RESULTS

In four different experiments, 33 mice were studied (table 1). Complete pathological analysis was performed in 25 mice (table 1). Disease incidence varied between 50 and 100% in different experiments (table 1). Our clinical observations were largely similar to those previously reported.⁷ Joint swelling, joint stiffness as demonstrated by loss of grip function on the cage grid, and joint deformity were the major symptoms (table 1). We also noticed an abnormal position of the nail in affected animals suggesting specific involvement of the nail bed and/or distal phalanx. At the end of the observation period 26/66 paws (39%) appeared normal. A score 1 (one toe affected)⁷ was given to 10/66 paws (15%), a score 2 (more than one toe affected) was assigned to 6/66 paws (9%). Progressive disease as demonstrated by loss of grip function due to toe stiffness (score 3) was found in 11/66 (17%) paws. Ankle arthritis or persisting deformity of a toe (score 4) was seen in 13/66 paws (20%). In addition, nail involvement was noticed in 8/66 (12%) paws.

Three different manifestations of the disease were recognised by microscopic analysis (table 1). Typical signs of AE characterised by endochondral bone formation were similar

Abbreviations: AE, ankylosing enthesitis; OPP, onychoprosperiostitis; PsA, psoriatic arthritis; SpA, spondyloarthropathy; SpAD, spontaneous arthritis in aging male DBA/1 mice

Table 1. Clinical and pathological evaluation of spontaneous arthritis in aging male DBA/1 mice			
Parameter	Score	Number of mice	Percentage
Onset of arthritis (weeks)	8-10	10	100
Number of joints affected	2-10	10	100
Duration of disease (weeks)	2-10	10	100
Number of joints affected (at 10 weeks)	2-10	10	100
Score 1: no arthritis	0	0	0
Score 2: mild arthritis	1	1	10
Score 3: moderate arthritis	2	2	20
Score 4: severe arthritis	3	3	30
Score 5: persistent deformity	4	4	40
Score 6: severe deformity	5	5	50
Score 7: severe deformity	6	6	60
Score 8: severe deformity	7	7	70
Score 9: severe deformity	8	8	80
Score 10: severe deformity	9	9	90
Score 11: severe deformity	10	10	100
Score 12: severe deformity	11	11	110
Score 13: severe deformity	12	12	120
Score 14: severe deformity	13	13	130
Score 15: severe deformity	14	14	140
Score 16: severe deformity	15	15	150
Score 17: severe deformity	16	16	160
Score 18: severe deformity	17	17	170
Score 19: severe deformity	18	18	180
Score 20: severe deformity	19	19	190
Score 21: severe deformity	20	20	200
Score 22: severe deformity	21	21	210
Score 23: severe deformity	22	22	220
Score 24: severe deformity	23	23	230
Score 25: severe deformity	24	24	240
Score 26: severe deformity	25	25	250
Score 27: severe deformity	26	26	260
Score 28: severe deformity	27	27	270
Score 29: severe deformity	28	28	280
Score 30: severe deformity	29	29	290
Score 31: severe deformity	30	30	300
Score 32: severe deformity	31	31	310
Score 33: severe deformity	32	32	320
Score 34: severe deformity	33	33	330
Score 35: severe deformity	34	34	340
Score 36: severe deformity	35	35	350
Score 37: severe deformity	36	36	360
Score 38: severe deformity	37	37	370
Score 39: severe deformity	38	38	380
Score 40: severe deformity	39	39	390
Score 41: severe deformity	40	40	400
Score 42: severe deformity	41	41	410
Score 43: severe deformity	42	42	420
Score 44: severe deformity	43	43	430
Score 45: severe deformity	44	44	440
Score 46: severe deformity	45	45	450
Score 47: severe deformity	46	46	460
Score 48: severe deformity	47	47	470
Score 49: severe deformity	48	48	480
Score 50: severe deformity	49	49	490
Score 51: severe deformity	50	50	500
Score 52: severe deformity	51	51	510
Score 53: severe deformity	52	52	520
Score 54: severe deformity	53	53	530
Score 55: severe deformity	54	54	540
Score 56: severe deformity	55	55	550
Score 57: severe deformity	56	56	560
Score 58: severe deformity	57	57	570
Score 59: severe deformity	58	58	580
Score 60: severe deformity	59	59	590
Score 61: severe deformity	60	60	600
Score 62: severe deformity	61	61	610
Score 63: severe deformity	62	62	620
Score 64: severe deformity	63	63	630
Score 65: severe deformity	64	64	640
Score 66: severe deformity	65	65	650
Score 67: severe deformity	66	66	660
Score 68: severe deformity	67	67	670
Score 69: severe deformity	68	68	680
Score 70: severe deformity	69	69	690
Score 71: severe deformity	70	70	700
Score 72: severe deformity	71	71	710
Score 73: severe deformity	72	72	720
Score 74: severe deformity	73	73	730
Score 75: severe deformity	74	74	740
Score 76: severe deformity	75	75	750
Score 77: severe deformity	76	76	760
Score 78: severe deformity	77	77	770
Score 79: severe deformity	78	78	780
Score 80: severe deformity	79	79	790
Score 81: severe deformity	80	80	800
Score 82: severe deformity	81	81	810
Score 83: severe deformity	82	82	820
Score 84: severe deformity	83	83	830
Score 85: severe deformity	84	84	840
Score 86: severe deformity	85	85	850
Score 87: severe deformity	86	86	860
Score 88: severe deformity	87	87	870
Score 89: severe deformity	88	88	880
Score 90: severe deformity	89	89	890
Score 91: severe deformity	90	90	900
Score 92: severe deformity	91	91	910
Score 93: severe deformity	92	92	920
Score 94: severe deformity	93	93	930
Score 95: severe deformity	94	94	940
Score 96: severe deformity	95	95	950
Score 97: severe deformity	96	96	960
Score 98: severe deformity	97	97	970
Score 99: severe deformity	98	98	980
Score 100: severe deformity	99	99	990
Score 101: severe deformity	100	100	1000

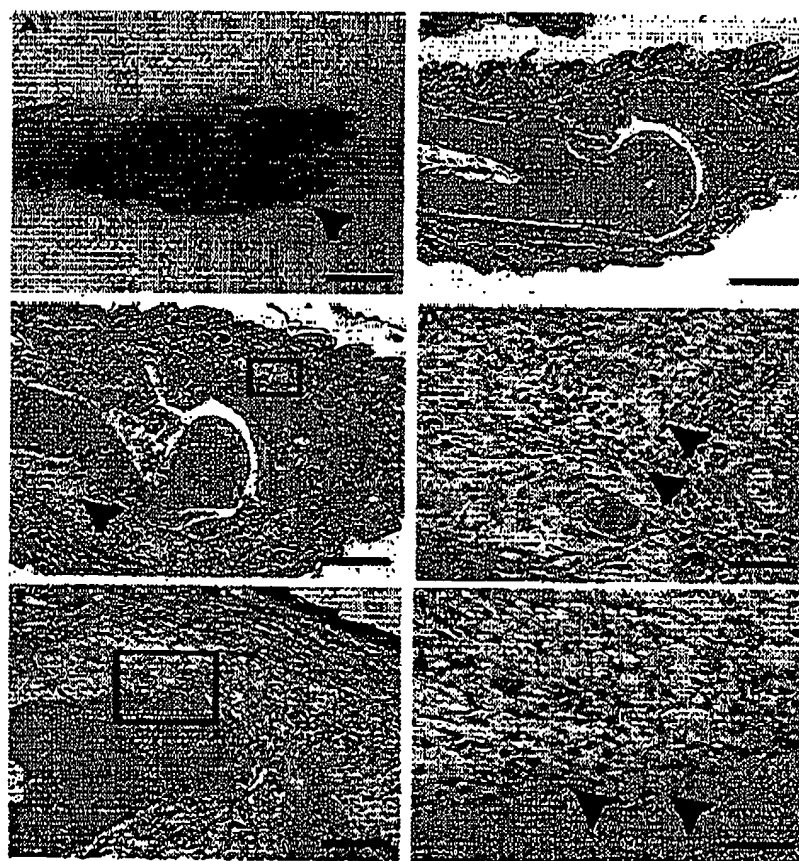


Figure 1. Dactylitis in spontaneous arthritis in aging male DBA/1 mice. (A) Clinical signs of dactylitis (swollen digit) in the 4th toe (arrowhead); (B) microscopic image of a normal toe with a proximal interphalangeal joint; (C) microscopic image of dactylitis showing extensive subcutaneous oedema and tenosynovitis with disruption of muscle and tendon fibres (arrowhead); (D) microscopic detail showing neutrophils (arrowheads) in the subcutaneous tissue; (E) inflammatory reaction adjacent to the enthesis; (F) microscopic detail showing polymorphonuclear and mononuclear cells (arrowheads) at the enthesis. (A) Bar = 2.5 mm. Haematoxylin and eosin staining; bar = 400 μ m (B, C), 200 μ m (E), and 50 μ m (D-F).

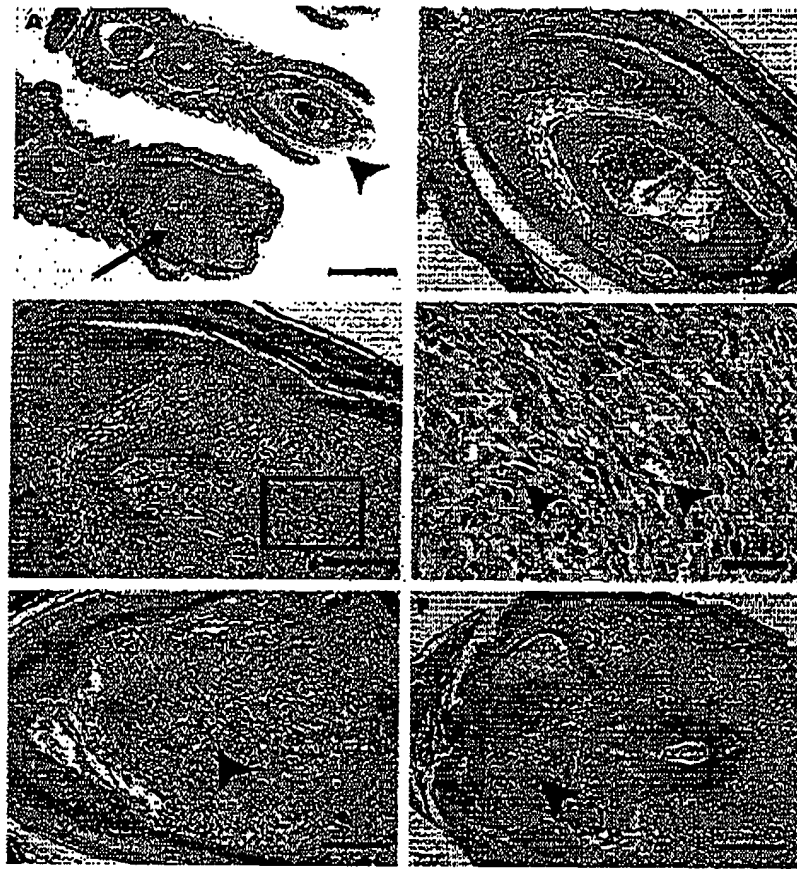


Figure 2 Onychoprositis in spontaneous arthritis in aging male DBA/1 mice. (A) Overview showing a normal toe and nail with the underlying distal phalanx (arrowhead) as well as a toe with an affected nail and distal phalanx periostitis (arrow); (B) detail of normal nail bed and distal phalanx; (C and E) periostitis in diseased nail showing a hypercellular tissue (C) and bone destructive, pannus-like tissue (E) invading the underlying distal phalanx (arrowhead); (D) detail from C showing spindle shaped cells and some small blood vessels (arrowheads); (F) late stage onychoprositis resulting in complete destruction of the nail bed and the distal phalanx (arrowhead). Haematoxylin and eosin staining; bar = 800 µm (A), 400 µm (F), 200 µm (B, C, E), and 50 µm (D).

to those previously reported.⁷ AE occurs rapidly. Already after 4 weeks of clinical symptoms abnormal cartilage and bone formation were found in 5/14 and 1/14 paws respectively (table 1). Eight weeks after clinical disease onset, cartilage formation was seen in 9/20 paws. Enthesial bone formation leading to joint space bridging was seen in 8/20 paws at this time (table 1).

We also noticed dactylitis and onychoprositis. The unexpected presence of dactylitis was noticed in 6/50 paws (table 1, fig 1). In contrast with the normal toes (fig 1B), the "sausage" digit was characterised by extensive subcutaneous oedema and an acute inflammatory reaction involving numerous neutrophils (figs 1C and D). No specific signs of inflammatory infiltrates within the synovium were recognised. In contrast, tenosynovitis with perimyscular and tendon sheath oedema as well as cell infiltration were seen (fig 1C, arrowhead). The overlying skin appeared normal. There were no signs of hyperkeratosis or dermal hyperplasia.

In two animals the acute inflammatory reaction apparently affected the enthesis itself, suggesting a link between the occurrence of dactylitis and AE (fig 1E). No inflammatory

cells were found within the fibrocartilage, but neutrophils, some mononuclear cells, and fibroblast-like cells were found at the border of the enthesis in close contact with the underlying bone and fibrocartilage (fig 1F).

In addition, sections through affected nails showed broadening of the nail base (fig 2A) and extensive cell proliferation above the distal phalanx, suggesting subonychia periosteal cell activation (fig 2C). Cells within this tissue mainly had a spindle shaped appearance and had prominent nucleoli (fig 2D). A few small blood vessels were found in the abnormal tissue (fig 2D). We found cells invading the bone, suggesting the presence of a periosteum derived, pannus-like tissue (fig 2E). In advanced stages the process of onychoprositis had led to the complete destruction of the distal phalanx and the overlying nail (fig 2F).

DISCUSSION

We have demonstrated AE, dactylitis, and onychoprositis in a spontaneous murine model of AE. These data further suggest common characteristics between the murine disease and human SpA and, in particular, PsA.

Dactylitis is a characteristic feature of PsA, encountered in about one third of patients at some stage in the disease.² It is more rarely recognised in other forms of SpA and seldom in sarcoidosis³ and tuberculosis.⁴ In accordance with our findings in the reported animal model, recent magnetic resonance imaging and ultrasound studies have suggested that diffuse digital oedema and flexor tenosynovitis are the hallmark features of dactylitis.^{5,6} McGonagle *et al* suggested that dactylitis may be caused by adjacent enthesitis.⁷ In the animals with dactylitis, however, no signs of synchronous AE or synovitis were seen. Similar data were recently reported in PsA using magnetic resonance imaging.⁸ Unlike other features of SpA, dactylitis may therefore not be linked to the enthesis. These new insights into dactylitis provide further evidence that PsA, in particular, cannot be explained by enthesitis alone.

AE with endochondral bone formation occurs rapidly in this animal model. Already within 4 weeks after clinical disease onset, not only extensive cartilage but also bone formation leading to joint space bridging is recognised. The number of joints affected steadily increases during the disease process. Eight weeks after clinical disease onset, most affected joints show signs of pathological bone formation, leading to joint space bridging and functional ankylosis. Although the mechanisms leading to AE are not clear, the possibility cannot be excluded that dactylitis triggers this process by the presence of an inflammatory reaction in proximity to the enthesis, as was suggested by our observations in two animals.

OPP has been described as a highly specific feature of PsA.⁹ Onychodystrophy, soft tissue swelling, and bone erosions of the distal phalanx typically characterise OPP. Our microscopy observations suggest that proliferative periostitis affects both the underlying bone and the overlying nail base in a continuous process. A similar mechanism may explain the strong relationship between distal interphalangeal joint arthritis/tenosynovitis and psoriatic nail involvement. Our observations are largely similar to the destructive inflammatory toe disease in different HLA transgenic mice lacking their own major histocompatibility complex.¹⁰

Remarkably, we did not see signs of skin involvement in DBA/1 mice. On the other hand, stress factors have an important role in SpAD as in human psoriasis and PsA. Grouping of male mice, causing a substantial level of stress and aggressive behaviour, is required for the development of disease.

We therefore conclude that SpAD shows some unexpected but very striking similarities to PsA. Therefore SpAD is not only an attractive model for studying the process of AE, in particular of pathological cartilage and bone formation, but

also for studying links between stress, inflammation, and pathological bone formation and for targeting specific genetic, metabolic, and inflammatory factors potentially relevant to PsA.

ACKNOWLEDGEMENTS

Rik Lories is the recipient of an "Aspirant" fellowship from the Fund for Scientific Research, Flanders. Patrick Mathys is the recipient of a post-doctoral fellowship from the Fund for Scientific Research, Flanders. This work was supported by research grant No G.0390.03 from the Fund for Scientific Research, Flanders.

Authors' affiliations

R J U Lories, K de Vlam, I Daeys, F P Luyten, Laboratory for Skeletal Development and Joint Disorders, Department of Rheumatology, University Hospitals Leuven, Katholieke Universiteit Leuven, Belgium
P Mathys, Laboratory for Immunobiology, Rega Institute, Katholieke Universiteit Leuven, Belgium

Correspondence to: Professor F P Luyten, Department of Rheumatology, University Hospitals Leuven, Herestraat 49, B-3000 Leuven, Belgium; Frank.Luyten@uz.kuleuven.ac.be

Accepted 26 July 2003

REFERENCES

- 1 Gledhill JD. Natural history of psoriatic arthritis. *Baillieres Clin Rheumatol* 1994;8:379-94.
- 2 Moll JM, Wright V. Psoriatic arthritis. *Semin Arthritis Rheum* 1973;3:65-78.
- 3 McGonagle D, Conaghan PG, Emery P. Psoriatic arthritis: a unified concept twenty years on. *Arthritis Rheum* 1999;42:1080-6.
- 4 Wright V. Seronegative polyarthritis: a unified concept. *Arthritis Rheum* 1978;21:619-33.
- 5 Goupille P, Lavielle J, Vachon V, Kaplan G, Vekic JP. Psoriatic ankyro- periostitis. Report of three cases. *Scand J Rheumatol* 1995;24:53-4.
- 6 Beissner-Gesmond AM, Boylat-Barry M, Douma AS, Boylat C, Baran R. Psoriatic onychopachydermoperiostitis. A variant of psoriatic distal interphalangeal arthritis? *Arch Dermatol* 1996;132:175-80.
- 7 Cantor A, Hassanz AS, Holmdahl R. T lymphocytes are not required for the spontaneous development of osteoarthral ossification leading to marginal ankylosis in the DBA/1 mouse. *Arthritis Rheum* 2000;43:844-51.
- 8 Nordling C, Karlsson-Porra A, Jonsson L, Holmdahl R, Menkes L. Characterization of a spontaneously occurring arthritis in mice DBA/1 mice. *Arthritis Rheum* 1992;35:717-22.
- 9 Pitt P, Hamilton CD, Lories RH, Marley KD, Monk BE, Hughes GR. Sarcoid dactylitis. *Ann Rheum Dis* 1993;42:634-9.
- 10 Wessels G, Hesselink PB, Beyer N. Skeletal tuberculosis dactylitis and involvement of the skull. *Radiat Radiol* 1998;28:234-6.
- 11 Olivieri L, Sakarini C, Carfisi F, Scammi E, Parikh A, Niccoli L, et al. Fast spin echo-T2 weighted sequences with fat saturation in dactylitis of spondyloarthritis. *Arthritis Rheum* 2002;46:2964-7.
- 12 Kase D, Groeney T, Bressanin B, Gibney R, Fitzgerald O. Ultrasonography in the diagnosis and management of psoriatic dactylitis. *J Rheumatol* 1999;26:1746-51.
- 13 Bardos T, Zhang J, Mitacek K, David CS, Glone TT. Mice lacking endogenous major histocompatibility complex class II develop arthritis resembling psoriatic arthritis at an advanced age. *Arthritis Rheum* 2002;46:2465-75.

nature

Altered thymic T-cell selection due to a mutation of the ZAP-70 gene causes autoimmune arthritis in mice

Noriko Sakaguchi^{*1,2}, Takeshi Takahashi^{*1}, Hiroshi Hata^{*1}, Takashi Nomura^{*1},
Tomoyuki Tagami^{*1}, Sayuri Yamazaki^{*1}, Toshiko Sakihama^{*1}, Takaji Matsutani^{*3},
Izumi Negishi^{*4}, Syuichi Nakatsuru^{*1} & Shimon Sakaguchi^{*1,2}

^{*1}*Department of Experimental Pathology, Institute for Frontier Medical Sciences, Kyoto University,
Kyoto 606-8507, Japan*

^{*2}*Laboratory for Immunopathology, RIKEN Research Center for Allergy and Immunology,
Yokohama 230-0045, Japan*

^{*3}*Department of Immunology, Shionogi Institute for Medical Science, Settsu, Osaka 566-0022, Japan*

^{*4}*Department of Dermatology, Gunma University Hospital, Maebashi, Gunma 371-8511, Japan*

Reprinted from Nature, Vol. 426, No. 6965, pp. 454–460, 27 November 2003

© Nature Publishing Group, 2003

Altered thymic T-cell selection due to a mutation of the ZAP-70 gene causes autoimmune arthritis in mice

Noriko Sakaguchi^{1,2*}, Takeshi Takahashi^{1*}, Hiroshi Hata¹, Takashi Nomura¹, Tomoyuki Tagami¹, Sayuri Yamazaki¹, Toshiko Sakihama¹, Takaji Matsutani³, Izumi Negishi⁴, Syuichi Nakatsuru¹ & Shimon Sakaguchi^{1,2}

¹Department of Experimental Pathology, Institute for Frontier Medical Sciences, Kyoto University, Kyoto 606-8507, Japan

²Laboratory for Immunopathology, RIKEN Research Center for Allergy and Immunology, Yokohama 230-0045, Japan

³Department of Immunology, Shionogi Institute for Medical Science, Settsu, Osaka 566-0022, Japan

⁴Department of Dermatology, Gunma University Hospital, Maebashi, Gunma 371-8511, Japan

* These authors contributed equally to this work

Rheumatoid arthritis (RA), which afflicts about 1% of the world population, is a chronic systemic inflammatory disease of unknown aetiology that primarily affects the synovial membranes of multiple joints¹⁻³. Although CD4⁺ T cells seem to be the prime mediators of RA, it remains unclear how arthritogenic CD4⁺ T cells are generated and activated¹⁻³. Given that highly self-reactive T-cell clones are deleted during normal T-cell development in the thymus, abnormality in T-cell selection has been suspected as one cause of autoimmune disease^{4,5}. Here we show that a spontaneous point mutation of the gene encoding an SH2 domain of ZAP-70, a key signal transduction molecule in T cells⁶, causes chronic autoimmune arthritis in mice that resembles human RA in many aspects. Altered signal transduction from T-cell antigen receptor through the aberrant ZAP-70 changes the thresholds of T cells to thymic selection, leading to the positive selection of otherwise negatively selected autoimmune T cells. Thymic production of arthritogenic T cells due to a genetically determined selection shift of the T-cell repertoire towards high self-reactivity might also be crucial to the development of disease in a subset of patients with RA.

The SKG strain, which spontaneously develops chronic arthritis, is derived from our closed breeding colony of BALB/c mice. Joint swelling with hyperaemia became macroscopically evident in SKG mice at about 2 months of age, initially at a few interphalangeal joints of the forepaws, then progressing in a symmetrical fashion to swelling of other finger joints of the forepaws and hindpaws, and larger joints (wrists and ankles) (Fig. 1a-d). Knee, elbow, shoulder or vertebral joints were rarely affected except for the joint at the base of the tail in aged SKG mice (Fig. 1e). Radiographic examination revealed destruction and fusion of the subchondral bones, joint dislocation, and osteoporosis by 8-12 months of age (Fig. 1f-i). Despite suffering from such severe chronic arthritis, most SKG mice survived well to 1 year of age, generally with more severe arthritides in females (Fig. 1j).

Histology of the swollen joints showed severe synovitis with massive subsynovial infiltration of neutrophils, lymphocytes, macrophages and plasma cells, villus proliferation of synoviocytes accompanying pannus formation and neovascularization, and neutrophil-rich exudates in the joint cavity (Fig. 1k, l), with progression of synoviocyte proliferation, pannus-eroded adjacent cartilage and subchondral bone. Immunohistochemical staining revealed that CD4⁺ T cells predominantly infiltrated the subsynovial tissue (Fig. 1m, n). As extra-articular manifestations of the disease, most (more than 90%) mice older than 6 months of age developed

interstitial pneumonitis with various degrees of perivascular and peribronchiolar cellular infiltration (Fig. 1o); more than 90% showed infiltration of inflammatory cells in the skin (Supplementary Fig. 1a). Some (10-20%) mice had subcutaneous necrobiotic nodules, not unlike rheumatoid nodules in RA (Fig. 1p), and vasculitides (Supplementary Fig. 1b). SKG mice did not show lymphadenopathy or lupus-like diseases (such as immune-complex glomerulonephritis).

SKG mice developed high titres of rheumatoid factor (RF), autoantibodies specific for type II collagen, antibodies reactive with heat shock protein (HSP)-70 of *Mycobacterium tuberculosis* presumably due to a cross-reaction with a conserved epitope of HSP, severe hypergammaglobulinaemia and a high concentration of the circulating immune complexes. However, there were no significant titres of anti-DNA antibodies or organ-specific autoantibodies such as those specific for thyroglobulins or gastric parietal cells^{1-3,7} (Fig. 1q-v).

Thus, this spontaneous arthritis in SKG mice resembles RA in clinical and histological characteristics of articular and extra-articular lesions and in serological features¹⁻³.

Transfer of spleen and lymph node T cells, CD4⁺ T cells in particular, from arthritic SKG mice produced similar arthritis in T-cell-deficient athymic BALB/c nude mice (Fig. 1w), whereas transfer of the sera from the same SKG mice did not (data not shown). Transfer of thymocyte suspensions from arthritic or non-arthritic young SKG mice also elicited severe arthritis in BALB/c nude mice and T/B-cell-deficient C.B-17 severe combined immunodeficiency (SCID) mice (Fig. 1x), whereas thymocyte transfer from normal BALB/c mice did not⁸. Furthermore, transfer of T-cell-depleted bone marrow cell suspensions from SKG mice produced severe arthritis in SCID mice, but not in SCID mice thymectomized before the transfer (Fig. 1x). These results collectively indicate that, first, the RA-like arthritis in SKG mice is a genuine autoimmune disease mediated by apparently joint-specific CD4⁺ T cells; second, the SKG thymus is continuously generating arthritogenic autoimmune T cells; and, third, the SKG bone marrow cells give rise to such arthritogenic T cells through the normal thymic environment, indicating that the arthritogenic abnormality in SKG mice is intrinsic to T cells.

The primary cause of the arthritis in SKG mice is a genetic abnormality, not vertical or horizontal transmission of arthritogenic microbes. The offspring of crosses between SKG and normal BALB/c mice, whether the mother was SKG or BALB/c, developed no arthritis (Fig. 2a). In contrast, arthritis with a clinical course and severity similar to that in SKG mice occurred in about 50% of the N₂ generation obtained by crossing the non-arthritic F₁ hybrids with SKG. Thus, the genetic abnormality was presumably of a single gene locus (designated the *skg* gene) and inherited in an autosomal recessive fashion with nearly 100% penetrance of the trait in homozygotes raised in our conventional environment.

Linkage analysis between the development of macroscopically evident arthritis and the homozygosity of chromosome-specific microsatellite markers, performed by using the N₂ generation with *Mus musculus castaneus* (CAST/Ei) (that is, SKG × (SKG × CAST/Ei)F₁ mice), mapped the *skg* locus to the centromeric portion of chromosome 1 with the lod score of the locus as infinite (Fig. 2b). Another significant linkage was with the region around the H-2 locus on chromosome 17 (Fig. 2c). This linkage was observed only when the mice were maintained in a nearly specific-pathogen-free (SPF) condition, but not in arthritis-prone non-SPF conventional condition (lod scores at the D17Mit28 locus: 2.95 in SPF compared with 0.40 in non-SPF). In the former condition, homozygosity of the H-2^d haplotype conferred higher genetic susceptibility to the arthritis, indicating that a polymorphism of the major histocompatibility complex (MHC) gene or the gene(s) linked to it can contribute to determining the susceptibility depending on the environmental conditions.

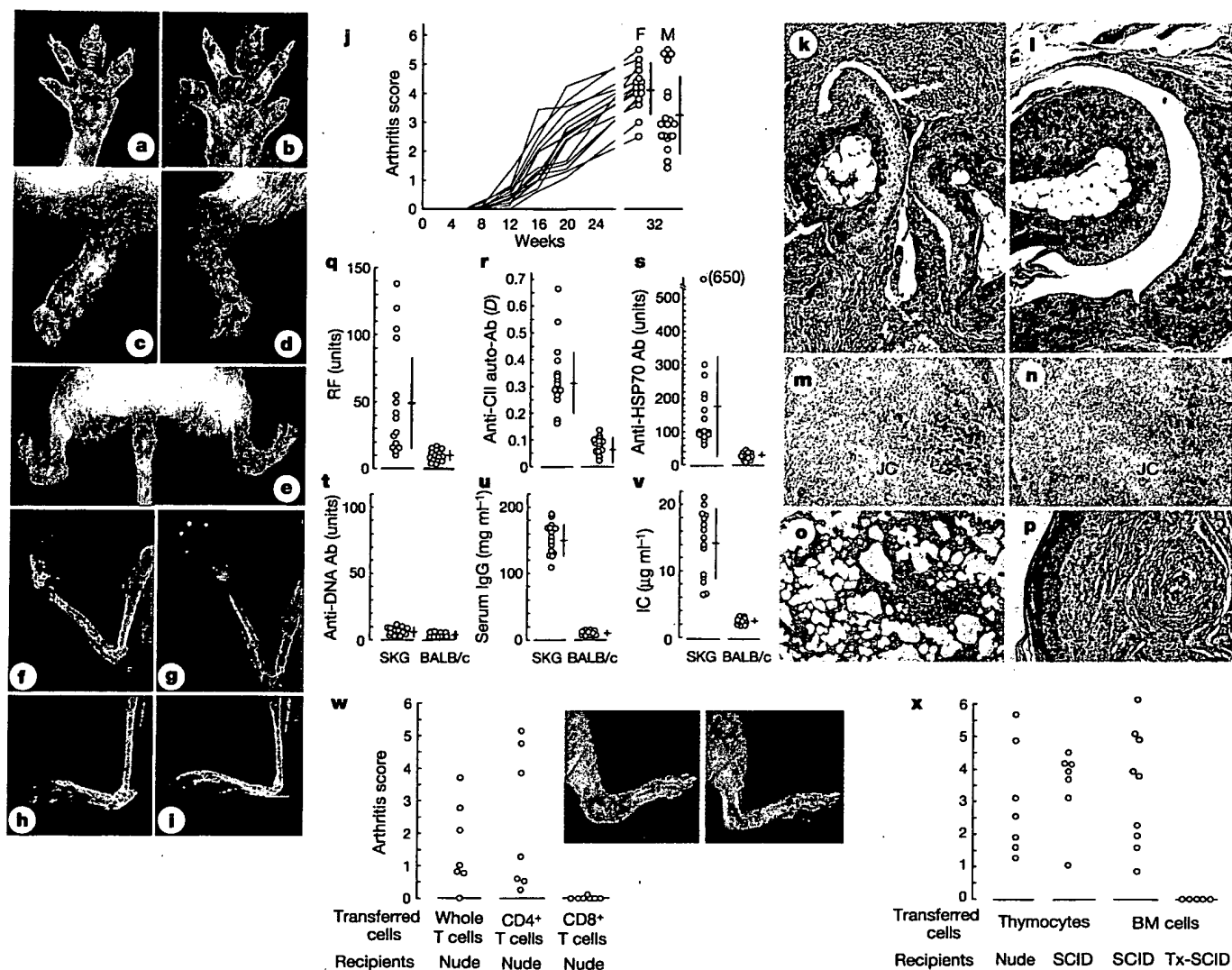


Figure 1 Arthritis in SKG mice. **a-e**, Swelling of joints: fingers (**a**) and toes (**b**) of a 4-month-old SKG mouse; forepaw (**c**) and hindpaw (**d**) of a 6-month-old SKG mouse; deformity of bilateral ankles and swelling of the base of the tail (**e**) in an 18-month-old SKG mouse. **f-i**, X-ray photographs of joints: wrist (**f**) and ankle (**h**) of an 8-month-old SKG mouse, and wrist (**g**) and ankle (**i**) of an 8-month-old BALB/c mouse. **j**, Time course of joint swelling in female SKG mice, and arthritis scores of 8-month-old female (F) and male (M) SKG mice ($n = 15$ each). Vertical bars represent s.e.m. See Methods for details on the scoring of joint swelling. **k-p**, Histology of arthritis and extra-articular lesions in SKG mice: a finger joint of a 6-month-old SKG (**k**) or BALB/c mouse (**l**) (haematoxylin/eosin (HE) staining, original magnification $\times 40$); immunoperoxidase staining of synovial tissue in a finger joint of a 3-month-old SKG mouse with anti-CD4 mAb (GK1.5) (**m**) or anti-CD8 mAb (3-155) (**n**) (magnification $\times 40$) (JC, joint cavity); interstitial pneumonitis (**o**) and a rheumatoid nodule-like lesion (**p**) in an 8-month-old SKG mouse (HE staining, magnification $\times 40$). **q-v**, Serological characteristics of SKG mice: RF (**q**), anti-CII Ab (**r**),

anti-HSP70 antibody (Ab) (**s**), anti-DNA antibody (**t**), concentration of IgG (**u**) and immune complexes (**v**) in the sera from 6-month-old female SKG or BALB/c mice ($n = 15$ each). **w**, Adoptive transfer of arthritis. The same dose (2.5×10^7) of whole, CD4⁺ or CD8⁺ T cells prepared from lymph nodes and spleens of arthritis-bearing 6-month-old SKG mice were transferred to 6-week-old BALB/c nude mice (SLC, Shizuoka). Inset, swelling of a hindpaw (left) and an intact paw (right) of a nude mouse transferred with CD4⁺ T cells and with CD8⁺ T cells, respectively. **x**, Thymocytes (10^6) or T-cell-depleted bone marrow cell suspensions (5×10^6) from the same SKG mice were transferred to 6-week-old nude or C.B.-17 SCID mice (Clea, Tokyo) or SCID mice that had been thymectomized 1 week after birth (Tx-SCID). The severity of arthritis in these mice was assessed 3 months later. CD4⁺ or CD8⁺ T cells were prepared by MACS (Miltenyi Biotec) with more than 95% purity. Bone marrow cells were treated with anti-Thy-1, anti-CD4 and anti-CD8 antibody and rabbit complement before transfer¹⁹.

To identify the *skg* gene, we then constructed a high-resolution genetic map of the *skg* region by using 1,352 mice with arthritis among a total of 2,939 N₂ mice (Fig. 2d). The mapping localized the *skg* locus to a 0.37-cM interval between two simple sequence-length polymorphism markers (nos 176-15 and 423-2), covered by two yeast artificial chromosomes (YACs) and ten bacterial artificial chromosomes (BACs) (Fig. 2d, top). Sequencing of several of these BACs localized the ZAP-70 gene on BAC no. 160. Sequencing of the entire coding region of ZAP-70 cDNA from SKG mice and comparison of the sequence with that of BALB/c mice revealed a

homozygous G-to-T substitution at nucleotide 489 in the SKG ZAP-70 gene, which altered codon 163 from tryptophan to cysteine (W163C) (Fig. 2d, bottom). This nucleotide substitution existed in the genomic DNA of SKG mice but not in other strains (see legend to Fig. 2). The position of the mutation corresponds to the initial amino-acid residue of the carboxy-terminal SH2 (SH2C) domain of ZAP-70 (Fig. 2d, inset).

To confirm that the ZAP-70^{W163C} mutation was primarily responsible for SKG arthritis, we crossed SKG mice, which had a ZAP-70^{skg/skg} genotype, with the heterozygotes of ZAP-70-deficient

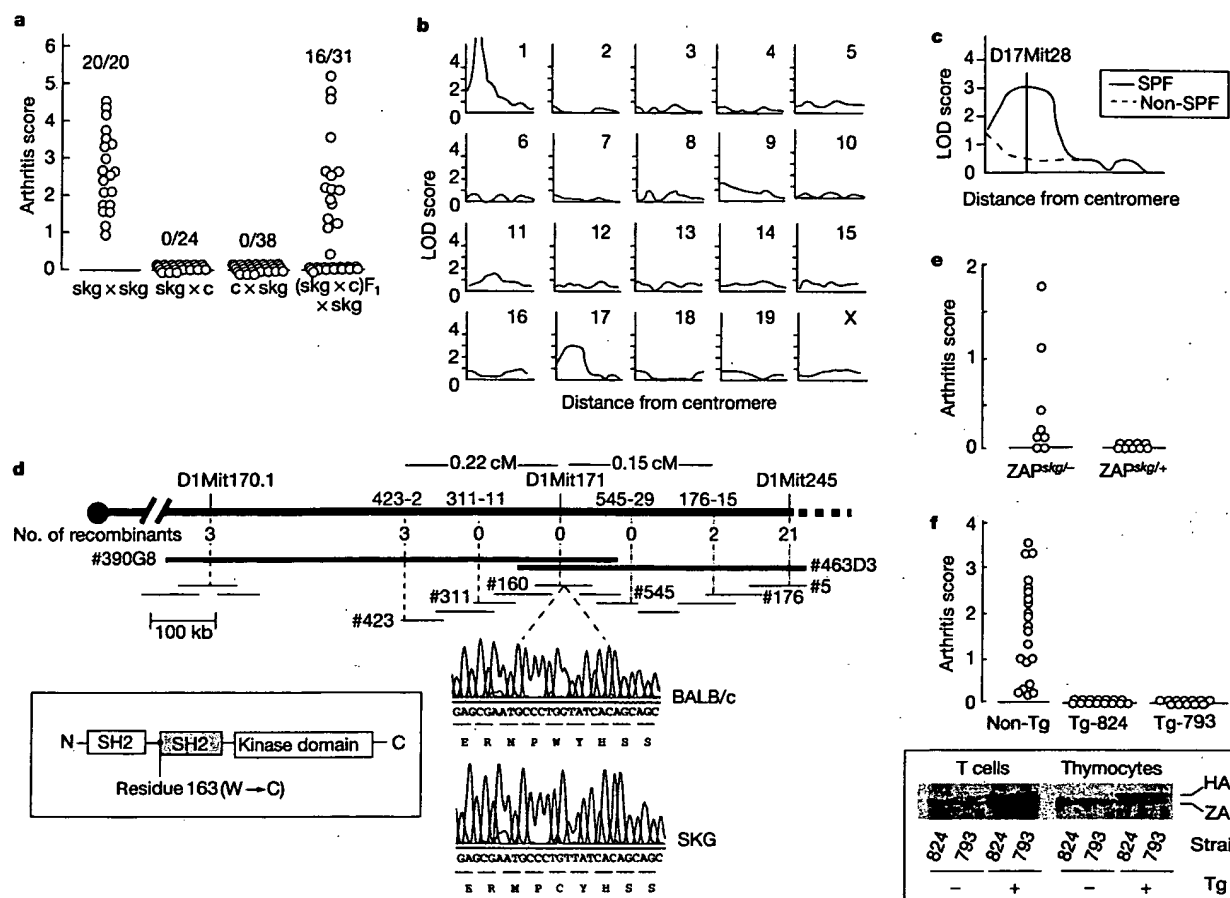


Figure 2 Genetic study of SKG arthritis. **a**, Autosomal recessive inheritance of SKG arthritis. skg \times skg, F_1 of mating SKG females with SKG males; skg \times c and c \times skg, F_1 of mating SKG females with BALB/c males, and BALB/c females with SKG males, respectively; (skg \times c) F_1 \times skg, N_2 mice of backcrossing (SKG \times BALB/c) F_1 mice with SKG mice. **b**, Genome-wide mapping of the *skg* locus. The LOD score curves were obtained by genotyping 58 arthritis-bearing N_2 mice by detecting microsatellite markers (Mouse MapPairs) locating every ~ 10 cM interval on each chromosome, in accordance with the manufacturer's instruction (Research Genetics). Chromosomes are identified with a number or X in each panel. **c**, Contribution of the loci on chromosome 17 to genetic susceptibility to SKG arthritis in a SPF condition. **d**, Genetic map of the *skg* locus on chromosome 1 with the number of recombinants and physical map of the locus with YAC

and BAC clones. Inset shows the structure of the ZAP-70 protein and the position of the *skg* mutation. The ZAP-70^{W163C} mutation in SKG mice was not found in other mouse strains including C57BL/6, C3H, DBA/1, DBA/2, 129^{Ter}/SV, FvB/N, NOD, MRL-lpr, NZW and CAST/Ei. **e**, SKG mice were mated with heterozygotes of ZAP-70-deficient mice, and the resulting ZAP-70^{skg/-} or ZAP-70^{skg/+} mice were assessed for joint swelling at 5 months of age. **f**, Rescue of SKG arthritis by expressing human normal ZAP-70 transgene⁹. The arthritis score of Tg-824 or Tg-793 mice, which were backcrossed three times to SKG mice, was assessed at 8 months of age. The expression of transgene-derived human ZAP-70 protein with HA-tag was assessed by western blotting with antibody against human ZAP-70 (Santa Cruz Biotech).

mice (ZAP-70^{+/-}) to produce mice with a ZAP-70^{skg/+} or ZAP-70^{skg/-} genotype⁹ and assessed the development of arthritis in these mice (Fig. 2e). Most of the ZAP-70^{skg/-} mice developed arthritis spontaneously by 3 months of age, in contrast with no arthritis in the ZAP-70^{skg/+} mice. Other immunological abnormalities of T cells and thymocytes were also similar between SKG mice and ZAP-70^{skg/-} mice but these were corrected in ZAP-70^{skg/+} mice (Supplementary Fig. 2a, and see below). Furthermore, transgenic (Tg) expression of the normal human ZAP-70 gene in SKG mice under the *lck* proximal promoter, which resulted in specific expression of the Tg ZAP-70 protein in thymocytes and peripheral T cells in two Tg lines, completely inhibited the development of arthritis and corrected other immunological abnormalities, contrasting with 100% incidence of arthritis in non-Tg littermates (Fig. 2f and Supplementary Fig. 2b).

Taken together, these results indicate that the ZAP-70^{W163C} alteration is not a mere polymorphism but is the causative mutation of SKG arthritis.

To determine, then, how the ZAP-70 mutation affects T-cell signal transduction, we assessed thymocytes and T cells from SKG or BALB/c mice for the tyrosine-phosphorylation status of major signal transduction molecules, including ZAP-70, TCR- ζ , LAT and PLC- γ 1 (refs 6, 10–12; Fig. 3a, b). After stimulation with anti-CD3 monoclonal antibody (mAb), the levels of phosphorylation of these molecules were extremely low in SKG thymocytes and T cells. Calcium mobilization, one of the earliest events induced by TCR stimulation, was also greatly impaired in SKG thymocytes and T cells, presumably because of the decreased phosphorylation of PLC- γ 1 (Fig. 3c). Immunoprecipitation of ZAP-70 from stimulated SKG thymocytes or T cells failed to co-precipitate tyrosine-phosphorylated p21 and p23 isoforms of TCR- ζ , indicating defective interactions between ZAP-70 and TCR- ζ ^{10,11} (Fig. 3b). Furthermore, downstream mitogen-activated protein (MAP) kinase signalling pathways involving ERK, JNK and p38 MAP kinases were also attenuated in SKG thymocytes¹³ (Supplementary Fig. 3). SKG T cells showed no enhancement of the expression of Syk,

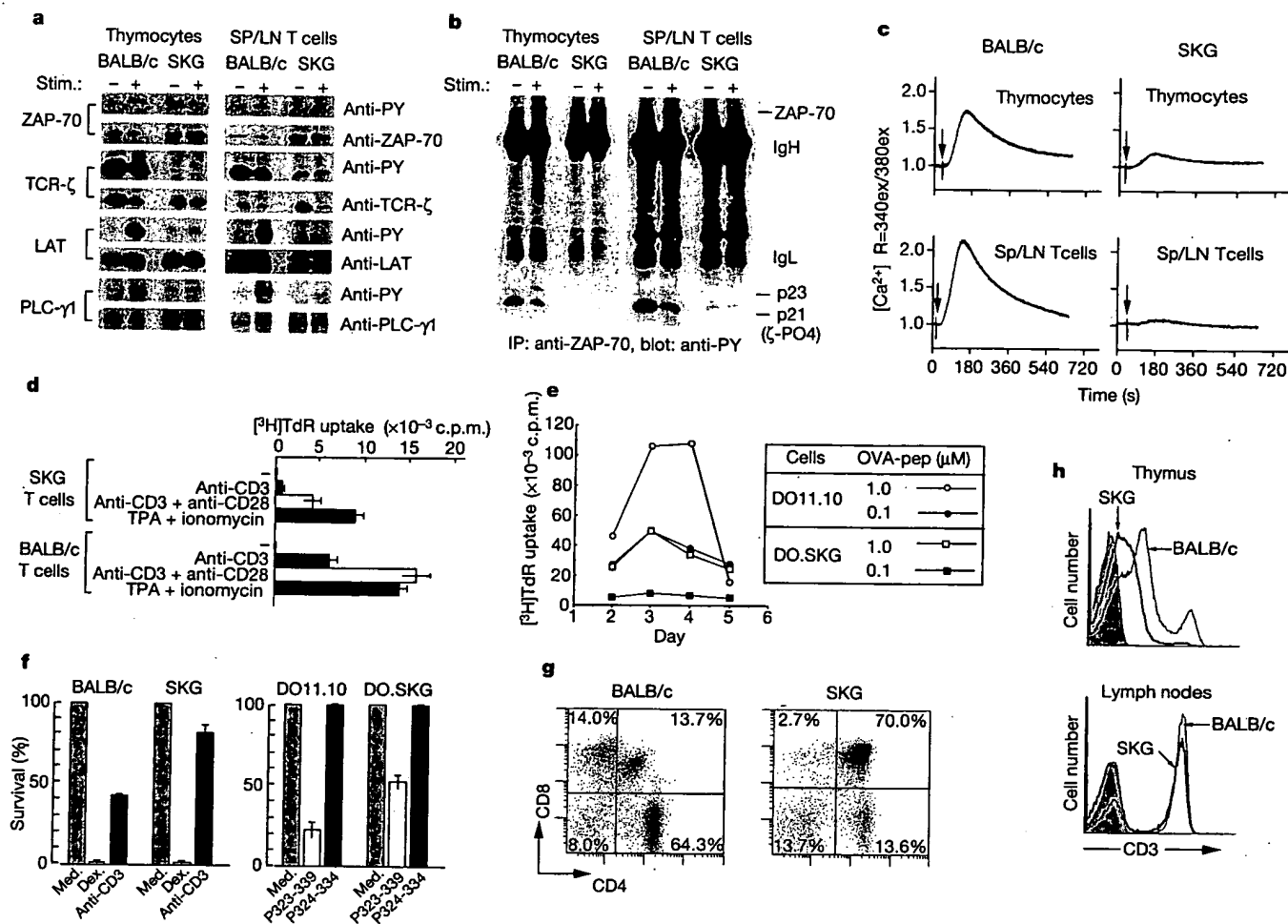


Figure 3 T-cell abnormalities in SKG mice. **a**, Impaired TCR signal transduction in SKG mice. Tyrosine phosphorylation status was assessed by immunoprecipitation and western blotting for ZAP-70, TCR- ζ , LAT and PLC- γ after anti-CD3 mAb stimulation of SKG or BALB/c thymocytes or spleen and lymph node (SP/LN) T cells. **b**, Association between ZAP-70 and TCR- ζ after CD3 crosslinking in SKG T cells and thymocytes. IP, immunoprecipitation. **c**, Ca²⁺ mobilization in SKG T cells or thymocytes after TCR stimulation. **d**, Proliferative responses of SKG T cells to various T-cell stimulations. **e**, Proliferation of CD4⁺ T cells from DO11.10 or DO.SK.G mice stimulated with the indicated concentrations of ovalbumin (OVA) peptides in the presence of BALB/c antigen-

presenting cells. **f**, Apoptosis of SKG or BALB/c thymocytes cultured with medium alone (med.), anti-CD3 mAb (2C11, 1 μ g ml⁻¹) or dexamethasone (Dex.) (100 nM) (left); apoptosis of DO11.10 or DO.SK.G thymocytes cultured with medium alone or indicated ovalbumin peptides (1 μ M) (right), as described previously⁹. **g**, Apoptosis of thymocytes in SKG or BALB/c mice injected intraperitoneally with anti-CD3 mAb (2C11; 250 μ g) 3 days previously⁹. These figures represent three independent experiments. **h**, Staining of thymocytes or lymph-node cells from a 2-month-old SKG or BALB/c mouse with anti-CD3 mAb.

another protein tyrosine kinase that might compensate for the role of ZAP-70 in T cells¹⁴ (T.T., unpublished data). These results collectively indicate that the ZAP-70^{W163C} mutation might impair the recruitment and association of ZAP-70 to tyrosine-phosphorylated immunoreceptor tyrosine-based activation motifs (ITAMs) of TCR- ζ and CD3 chains, thereby altering signal transduction through ZAP-70.

In accord with this attenuated signal transduction through ZAP-70, SKG T cells were hyporesponsive to polyclonal TCR stimulation *in vitro*, for example with anti-CD3 mAb, whereas they responded well to stimulation by 12-O-tetradecanoylphorbol-13-acetate (TPA) and ionomycin, which transduces a signal to TCR-distal pathways (Fig. 3d). When the *skg* gene was homozygously introduced to DO11.10 TCR-Tg mice, in which most T cells express Tg TCRs specific for an ovalbumin peptide¹⁵, T cells from such mice (designated DO.SK.G mice) required a peptide concentration 10-fold that in DO11.10 T cells to exhibit an equivalent magnitude of proliferation (Fig. 3e). Furthermore, SKG thymocytes

were resistant to apoptosis induced by TCR stimulation, but not to dexamethasone-induced apoptosis, as shown by the stimulation of SKG or DO.SK.G thymocytes *in vitro* with anti-CD3 mAb or the specific peptide, respectively (Fig. 3f), or by inoculation with anti-CD3 mAb *in vivo* (Fig. 3g).

SKG mice were also aberrant in T-cell development. In comparison with normal BALB/c mice, TCR^{high} mature thymocytes decreased in number and ratio, whereas TCR^{low} immature thymocytes increased in the SKG thymus; the levels of TCR expression on mature thymocytes or peripheral T cells were comparable between the two strains (Fig. 3h). The numbers of peripheral CD4⁺ and CD8⁺ T cells consequently decreased in SKG mice, with a relative increase in B cells (Supplementary Fig. 4). There was no significant difference in the total number of thymocytes or spleen cells, the thymic architecture, the number and function of natural killer cells (which express ZAP-70) or the composition of T-cell subpopulations expressing particular TCR V α or V β families (Supplementary Fig. 5).

We then assessed the effects of the *skg* mutation on thymic positive and negative selection by introducing the *skg* gene homozygously into TCR-Tg mice^{15,16}. In DO.SKG (that is, DO^{skg/skg}) mice, the number of CD4⁺CD8⁻ mature thymocytes decreased to ~20% of normal DO11.10 mice (Fig. 4a). Furthermore, only ~30% of CD4⁺CD8⁻ thymocytes were Tg-TCR^{high} (when stained with clonotype-specific KJ1-26 mAb)¹⁵ in contrast to ~80% in DO11.10 mice (Fig. 4a, b); the rest of CD4⁺CD8⁻ thymocytes (that is, KJ1-26^{low}, hence Tg-TCR^{low} thymocytes) in DO^{skg/skg} mice seemed to express endogenous TCR α -chains. Similarly, Tg-TCR^{high} T cells constituted only ~30% of CD4⁺ T cells in the periphery of DO^{skg/skg} mice, contrasting with ~70% in DO11.10 mice (Fig. 4a, b); Tg-TCR^{low} T cells in DO^{skg/skg} mice expressed endogenous α -chains associated with transgenic β -chains (Supplementary Fig. 6). In *skg*-heterozygous DO^{skg/+} mice, the decrease or increase in the percentage of Tg-TCR^{high} or Tg-TCR^{low} T cells, respectively, in the thymus and the periphery was intermediate between that in the DO^{skg/skg} and that in DO11.10 mice (Fig. 4a, b).

In HY-TCR Tg mice that express transgenic TCRs specific for male-specific HY antigens on an H-2^b background, female HY-TCR Tg mice positively selected HY-TCR⁺CD8⁺CD4⁻ thymocytes (detected by clonotype-specific T3.70 mAb)¹⁶. In contrast, female HY-TCR Tg mice with the homozygous *skg* gene (designated HY-TCR.SKG Tg mice) on an H-2^b background hardly showed any positive selection of HY-TCR⁺CD8⁺CD4⁻ thymocytes and T cells¹⁷ (Fig. 4c). However, in contrast to substantial deletion of HY-TCR⁺CD8⁺CD4⁻ thymocytes in male HY-TCR Tg mice, male

HY-TCR.SKG Tg mice showed efficient positive selection of HY-TCR⁺CD8⁺CD4⁻ thymocytes in almost a comparable number to those in female HY-TCR Tg mice. Furthermore, HY-TCR⁺ peripheral T cells in male HY-TCR.SKG Tg mice expressed nearly normal levels of CD8 expression, contrasting with low-level CD8 expression in male HY-TCR Tg mice¹⁶.

Both DO.SKG and HY-TCR.SKG mice developed arthritis at high incidences (Fig. 4d). Transfer of Tg-TCR^{low} cells (as KJ1-26^{low} cells) from such arthritis-bearing DO.SKG mice to C.B-17 SCID mice induced arthritis, whereas transfer of Tg-TCR^{high} cells did not (Fig. 4e), indicating that TCR-Tg mice with the *skg* mutation positively select arthritogenic T cells expressing endogenous TCR α -chains paired with transgenic β -chains (see above).

Taken together, these results show that the *skg* mutation alters the sensitivity of developing thymocytes to both positive and negative selection, thereby leading to positive selection of otherwise negatively selected autoimmune T cells. This recessive mutation affects T-cell selection even in the heterozygotes, although to a smaller degree than in the homozygotes. Furthermore, the degree of impairment in T-cell signal transduction through ZAP-70 can determine the degree of thymic positive or negative selection, and consequently the phenotype of immunological diseases. The *skg* mutation of the SH2C domain of ZAP-70 elicits autoimmune arthritis, whereas a mutation in the kinase domain of ZAP-70 leads to a severe impairment of positive selection and hence total T-cell deficiency¹⁸.

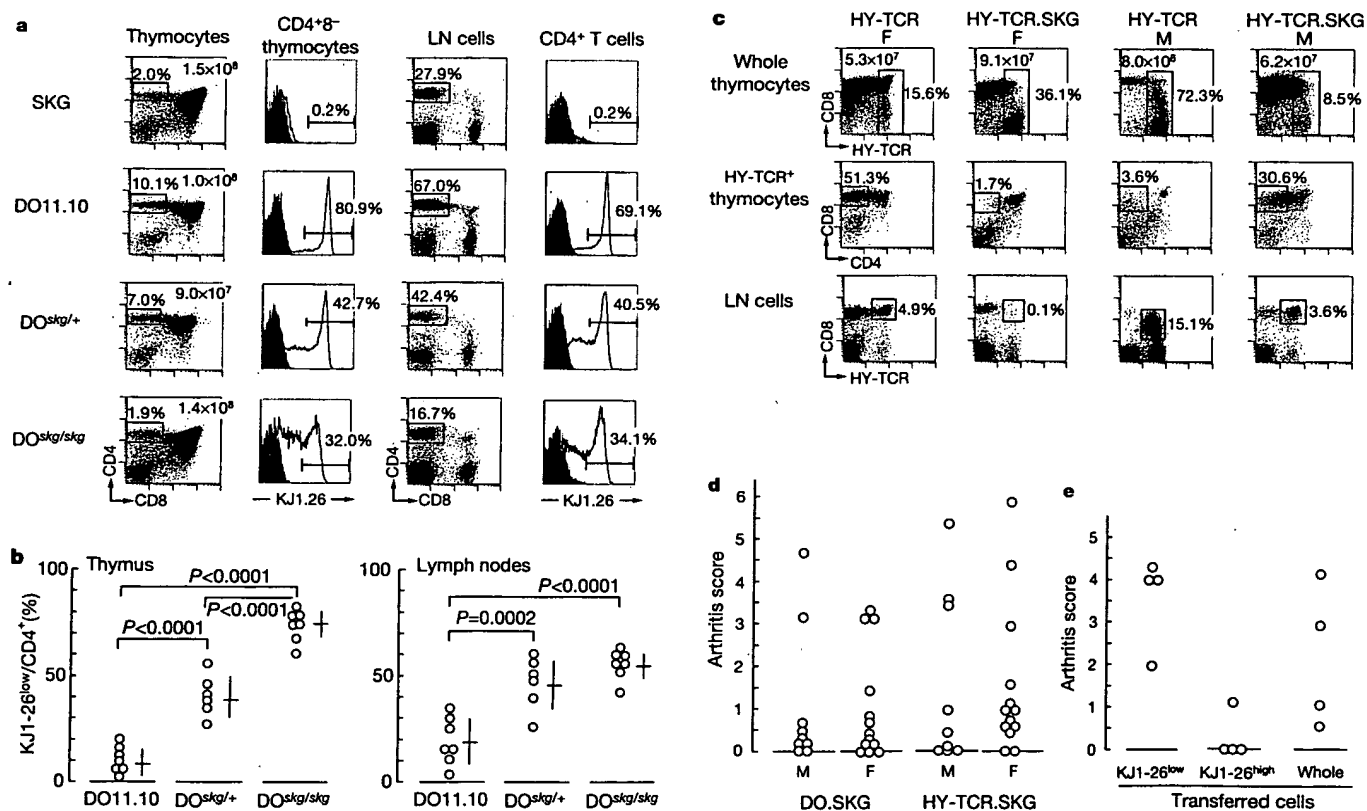


Figure 4 Altered thymic T-cell selection in SKG mice. **a**, Staining of thymocytes or lymph-node cells from a 4-month-old DO11.10, DO^{skg/skg} or DO^{skg/+} mouse with the indicated monoclonal antibodies. Dot-plot figures are scaled logarithmically. Ordinates of histograms denote cell number (arbitrary units). **b**, The percentage of KJ1-26^{low} T cells among CD4⁺CD8⁻ thymocytes or CD4⁺ T cells was also assessed for individual DO11.10, DO^{skg/+} or DO^{skg/skg} mice. **c**, Staining of thymocytes or lymph-node cells from a

4-month-old female or male HY-TCR or HY-TCR.SKG transgenic mouse with the indicated monoclonal antibodies. **d**, Arthritis scores of 6-month-old DO.SKG or HY-TCR.SKG mice. **e**, Adoptive transfer of arthritis from arthritis-bearing DO.SKG mice to SCID mice, which were assessed for joint swelling 2 months later. Each fraction of cells (10^6) was purified by cell sorter from CD4⁺ lymph node and spleen cells.

On the assumption that thymic positive and negative selection of developing T cells requires a certain range of TCR signal through ZAP-70, the *skg* mutation is likely to raise the threshold of TCR avidity for self-peptide/MHC ligands required for the selection to compensate for the reduced signal through the aberrant ZAP-70. This results in a 'selection shift' of the T-cell repertoire towards high reactivity to self-peptide/MHC ligands in the thymus, leading to the thymic production of highly self-reactive T cells that would not be produced by the normal thymuses of ZAP-70-intact animals. The pathogenic self-reactive T cells thus produced by the SKG thymus apparently overcome the mechanisms of peripheral self-tolerance, for example, mediated by naturally occurring CD25⁺CD4⁺ regulatory T cells^{8,19}. However, it remains to be determined whether the *skg* mutation might also alter the repertoire of CD25⁺CD4⁺ regulatory T cells or somehow affect their suppressive activity^{8,19}.

A critical question on SKG arthritis is why this general alteration in T-cell repertoire should lead to the predominant development of autoimmune arthritis but not other autoimmune diseases. In contrast with other organ-specific autoimmune diseases in which self-reactive T cells destroy the target cells (for example, type 1 diabetes due to destruction of insulin-secreting pancreatic β -cells), a cardinal feature of autoimmune arthritis in SKG mice (and also RA in humans) is that self-reactive T cells do not destroy synovio-cytes but stimulate them to proliferate¹⁻³. This is partly due to a high sensitivity of synovio-cytes to various stimuli that can activate them (as also illustrated by other arthritis models^{7,19-25}) and their distinct capacity to secrete proinflammatory cytokines (such as interleukin-1, interleukin-6 and tumour necrosis factor- α) and chemical mediators that destroy the surrounding cartilage and bone^{1-3,26,27}. It is therefore likely that this unique combination of a high and broad self-reactivity of SKG T cells and a high susceptibility of synovial cells to inflammatory stimuli (including T-cell self-reactivity) leads to predominant development of autoimmune arthritis in SKG mice.

Our findings indicate that mutations of other loci of the ZAP-70 gene or the genes encoding other signalling molecules especially at TCR proximal steps, even if they are heterozygous mutations, might contribute to the development of autoimmune disease by affecting thymic T-cell selection²⁸⁻³⁰. Indeed, we have recently found heterozygous mutations in the ITAM regions of the TCR- ζ chain gene in 2.5% of 160 RA patients in our hospital (H.H., N.S., S.N., T.N. and S.S., unpublished observations). Physical association between these mutated TCR- ζ chain molecules and the normal ZAP-70 molecules, assessed by surface plasmon resonance, was significantly lower than normal as observed between the mutated ZAP-70 in SKG mice and the normal TCR- ζ chain (T.N. and S.S., unpublished data). As RA is a heterogeneous disease with complex genetics¹⁻³, RA with a similar aetiology to SKG arthritis represents only a fraction of the disease. Nevertheless, further analyses of SKG arthritis at each step of the pathogenetic pathway from the ZAP-70 mutation, through thymic generation of autoimmune T cells, to the activation of arthritogenic T cells and inflammatory destruction of the joint, will explain how genetic and environmental factors contribute to the development of RA. This will help in the design of effective methods of detection, treatment and prevention of RA. □

Methods

Scoring of joint swelling

Joint swelling was monitored by inspection and scored as follows: 0, no joint swelling; 0.1, swelling of one finger joint; 0.5, mild swelling of wrist or ankle; 1.0, severe swelling of wrist or ankle. Scores for all fingers of forepaws and hindpaws, wrists and ankles were totalled for each mouse.

Enzyme-linked immunosorbent assay (ELISA)

Affinity-purified mouse IgG (5 μ g ml⁻¹), 10 μ g ml⁻¹ bovine type II collagen (Funakoshi), 5 μ g ml⁻¹ double or single-stranded-DNA, or 10 μ g ml⁻¹ HSP-70 of *Mycobacterium tuberculosis* in PBS, pH 7.2, were used for overnight coating of ELISA plates (Flow Laboratories)⁷⁴. Test sera were diluted 1:10 for anti-type II collagen or anti-HSP-70 assay,

1:20 for RF assay, or 1:40 for anti-DNA assay. Alkaline-phosphatase-conjugated anti-mouse IgG or IgM (for RF assay) (Southern Biotechnology Associates) was used at 1 μ g ml⁻¹ as the secondary reagent⁷⁴. Pooled serum from MRL-lpr mice was used as the standard of arbitrary units in the RF, anti-DNA or anti-HSP70 antibody assay⁷. The titre of anti-CII antibody was expressed as attenuation. The amount of immune complex was measured by anti-C3 assay; the serum concentration of IgG was measured by the single radial immunodiffusion method⁷.

In vitro T-cell activation

SKG or BALB/c T cells (3.0×10^6) were stimulated for 72 h with plate-bound anti-CD3 mAb (2C11) in the presence or absence of plate-bound anti-CD28 mAb in RPMI-1640 medium supplemented with 10% fetal calf serum and 50 μ M 2-mercaptoethanol. Cells were also stimulated with TPA (1.4 ng ml⁻¹) and ionomycin (0.14 μ M). KJ1.26⁺ T cells from DO or DO.SKG mice were stimulated with ovalbumin (323-339) peptide in the presence of X-irradiated syngeneic spleen cells (10^5 cells) as antigen-presenting cells in 96-well round-bottomed plates. The incorporation of [³H]thymidine by proliferating lymphocytes during the last 6 h of the culture was measured.

Immunoprecipitation and western blotting

Thymocytes or purified T cells (5×10^6) were incubated with anti-CD3 mAb (2C11) for 20 min, followed by cross-linking with antibody against Armenian hamster immunoglobulin (Jackson ImmunoResearch) (10 μ g ml⁻¹) at 37 °C for the indicated duration. For immunoprecipitation, cells were lysed with RIPA buffer (0.5% Triton X-100, 20 mM Tris-HCl pH 7.5, 1 mM EDTA, 150 mM NaCl, 20 mM NaF, 1 mM Na₃VO₄) supplemented with protease inhibitors. The immune complexes were recovered by Protein A-conjugated Sepharose beads. For western blot analyses, cells were directly lysed by sample-loading buffer for SDS-polyacrylamide gel electrophoresis (SDS-PAGE) and immediately boiled for 4 min. Recovered immune complexes or total cell lysates were subjected to SDS-PAGE and transferred to poly(vinylidene difluoride) membranes, which were blotted with various antibodies after being blocked with PBS/5% BSA. Antibodies specific for the following proteins were used: ZAP-70 (Santa Cruz Biotech), TCR- ζ (Santa Cruz Biotech), LAT (Upstate Biotechnology), PLC- γ 1 (Upstate Biotechnology), activated or total ERK1/2, SAPK/JNK and p38 MAP kinases (Cell Signalling Technology) or phosphotyrosine (4G10) (Upstate Biotechnology).

Calcium mobilization

Thymocytes or purified T cells were loaded with Fura-2 acetoxymethyl ester (Nacalai) for 30 min at 37 °C. Cells were then incubated with anti-CD3 mAb as described above, washed and resuspended with PBS. CaCl₂ was added to the samples 2 min before cross-linking cell surface-bound anti-CD3 mAb with anti-hamster antibody (Jackson ImmunoResearch). Fura-2 fluorescence was measured by a spectrofluorimeter (Nihon Bunkou).

Received 4 August; accepted 13 October 2003; doi:10.1038/nature02119.

- Harris, E. D. *Rheumatoid Arthritis* (W. B. Saunders, Philadelphia, 1997).
- Feldmann, M., Brennan, F. M. & Maini, R. N. Rheumatoid arthritis. *Cell* 85, 307-310 (1996).
- Firestein, G. F. in *Textbook of Rheumatology* 5th edn (eds Kelley, W. N., Ruddy, S., Harris, E. D. & Sledge, C. B.) 851-897 (W. B. Saunders, Philadelphia, 1997).
- Marrack, P., Kappler, J. & Kotzin, B. L. Autoimmune disease: why and where it occurs. *Nature Med.* 7, 899-905 (2001).
- von Boehmer, H. et al. Thymic selection revisited: how essential is it? *Immunol. Rev.* 191, 62-78 (2003).
- Chan, A. C., Iwashima, M., Turck, C. W. & Weiss, A. ZAP-70: a 70 kd protein-tyrosine kinase that associates with the TCR zeta chain. *Cell* 71, 649-662 (1992).
- Sakaguchi, S. & Sakaguchi, N. Thymus and autoimmunity: capacity of the normal thymus to produce pathogenic self-reactive T cells and conditions required for their induction of autoimmune disease. *J. Exp. Med.* 172, 537-545 (1990).
- Itoh, M. et al. Thymus and autoimmunity: production of CD25⁺ CD4⁺ naturally anergic and suppressive T cells as a key function of the thymus in maintaining immunologic self-tolerance. *J. Immunol.* 162, 5317-5326 (1999).
- Negishi, I. et al. Essential role for ZAP-70 in both positive and negative selection of thymocytes. *Nature* 376, 435-438 (1995).
- van Oers, N. S. et al. The 21- and 23-kD forms of TCR zeta are generated by specific ITAM phosphorylations. *Nature Immunol.* 1, 322-328 (2000).
- Iwashima, M. et al. Sequential interactions of the TCR with two distinct cytoplasmic tyrosine kinases. *Science* 263, 1136-1139 (1994).
- Zhang, W., Sloan-Lancaster, J., Kitchen, J., Triple, R. P. & Samelson, L. E. LAT: the ZAP-70 tyrosine kinase substrate that links T cell receptor to cellular activation. *Cell* 92, 83-92 (1998).
- Rincon, M. MAP-kinase signaling pathway in T cells. *Curr. Opin. Immunol.* 13, 339-345 (2001).
- Noraz, N. et al. Alternative antigen receptor (TCR) signaling in T cells derived from ZAP-70-deficient patients expressing high levels of Syk. *J. Biol. Chem.* 275, 15832-15838 (2000).
- Murphy, K. M., Heimberger, A. B. & Loh, D. Y. Induction by antigen of intrathymic apoptosis of CD4⁺CD8⁺TCR^{lo} thymocytes in vivo. *Science* 250, 1720-1723 (1990).
- Kisielow, P., Bluthmann, H., Staerz, U. D., Steinmetz, M. & von Boehmer, H. Tolerance in T-cell-receptor transgenic mice involves deletion of nonmature CD4⁺8⁺ thymocytes. *Nature* 333, 742-746 (1988).
- Kisielow, P., Teh, H. S., Bluthmann, H. & von Boehmer, H. Positive selection of antigen-specific T cells in thymus by restricting MHC molecules. *Nature* 335, 730-733 (1988).
- Wiest, D. L. et al. A spontaneously arising mutation in the DLAAARN motif of murine ZAP-70 abrogates kinase activity and arrests thymocyte development. *Immunity* 6, 663-671 (1997).
- Sakaguchi, S., Sakaguchi, N., Asano, M., Itoh, M. & Toda, M. Immunologic self-tolerance maintained

- by activated T cells expressing IL-2 receptor α -chains (CD25). Breakdown of a single mechanism of self-tolerance causes various autoimmune diseases. *J. Immunol.* 155, 1151–1164 (1995).
20. Keffe, J. *et al.* Transgenic mice expressing human tumor necrosis factor: a predictive genetic model of arthritis. *EMBO J.* 10, 4025–4031 (1991).
 21. Kouskoff, V. *et al.* Organ-specific disease provoked by systemic autoimmunity. *Cell* 87, 811–822 (1996).
 22. Pals, S. T., Radaszkiewicz, T., Roozendaal, L. & Gleichman, E. Chronic progressive polyarthritis and other symptoms of collagen vascular disease induced by graft-versus-host reaction. *J. Immunol.* 134, 1475–1482 (1985).
 23. Nishimura, H., Nose, M., Hiai, H., Minato, N. & Honjo, T. Development of lupus-like autoimmune diseases by disruption of the PD-1 gene encoding an ITIM motif-carrying immunoreceptor. *Immunity* 11, 141–151 (1999).
 24. Horai, R. *et al.* Development of chronic inflammatory arthropathy resembling rheumatoid arthritis in interleukin 1 receptor antagonist-deficient mice. *J. Exp. Med.* 191, 313–320 (2000).
 25. Atsumi, T. *et al.* A point mutation of Tyr-759 in interleukin 6 family cytokine receptor subunit gp130 causes autoimmune arthritis. *J. Exp. Med.* 196, 979–990 (2002).
 26. Dayer, J. M. & Burger, D. Cytokines and direct cell contact in synovitis: relevance to therapeutic intervention. *Arthritis Res.* 1, 17–20 (1999).
 27. Naka, T., Nishimoto, N. & Kishimoto, T. The paradigm of IL-6: from basic science to medicine. *Arthritis Res.* 4 (Suppl. 3), S233–S242 (2002).
 28. Werlen, G., Hausmann, B., Naecher, D. & Palmer, E. Signaling life and death in the thymus: timing is everything. *Science* 299, 1859–1863 (2003).
 29. Nambiar, M. P. *et al.* T cell signalling abnormalities in systemic lupus erythematosus are associated with increased mutations/polymorphisms and splice variants of T cell receptor zeta chain messenger RNA. *Arthritis Rheum.* 44, 1336–1350 (2001).
 30. Takeuchi, T. *et al.* TCR zeta chain lacking exon 7 in two patients with systemic lupus erythematosus. *Int. Immunol.* 10, 911–921 (1998).

Supplementary information accompanies the paper on www.nature.com/nature.

Acknowledgements We thank H. von Boemer for transgenic mice; M. Singh (GBF, Germany) for a gift of recombinant HSP-70 through the support of the UNDP/World Bank/WHO Special Program for Research and Training on Tropical Diseases; F. Melchers, R. Zinkernagel, K. Yamamoto, R. Suzuki and Z. Fehervari for discussion; A. Kosugi and T. Nakayama for reagents; and E. Moriizumi for immunohistochemistry and histology. This work was supported by grants-in-aid from the Ministry of Education, Science, Sports and Culture, the Ministry of Human Welfare, Japan Science and Technology Corporation, and the Organization for Pharmaceutical Safety and Research of Japan.

Authors' contributions The SKG strain was established by S.S. and N.S. The experiments in Figs 1, 2a–d, 3f–h, 4, Supplementary Figs 1, 4 and 6 were conducted by N.S. and S.S.; those in Fig. 2b–d by Ta.T., N.S., H.H., To.T., S.Y., T.S., S.N. and S.S.; those in Figs 2e, f, 3a–c, e and Supplementary Fig. 2 by Ta.T.; that in Fig. 3d by To.T.; that in Supplementary Fig. 3 by T.N., and that in Supplementary Fig. 5 by T.M. ZAP-70-deficient mice were provided by I.N.

Competing interests statement The authors declare that they have no competing financial interests.

Correspondence and requests for materials should be addressed to S.S. (shimon@frontier.kyoto-u.ac.jp).